

## Response to Reviewers

Determination of vadose and saturated-zone nitrate lag times using long-term groundwater monitoring data and statistical machine learning

Hydrol. Earth Syst. Sci. Discuss., <https://doi.org/10.5194/hess-2020-169>, 2020.

We are very grateful to Pia Ebeling for a detailed and helpful review of the paper. We are also grateful to the second reviewer, who reviewed the manuscript for the second time and had no further revisions to suggest.

The marked, revised manuscript is appended below.

In our responses, we tried to balance the new reviewer suggestions with those of previous reviewers as well as the overall genesis of the manuscript. We made one significant change (rearranging Sections 2.3-2.5 of the Methods), and several minor changes in line with reviewer comments. We were less responsive to the overriding theme of shortening the Methods section. We agree that it is possible to cut out some of the text in this paper and replace with references. At the same time, although machine learning (and RF in particular) is becoming much more common, there are still many hydrologists and practitioners who are unfamiliar with the methods (Saia et al., 2020). At least one reviewer specifically noted their appreciation for the additional detail. Finally, as an author group, we believe it is common for those who are intimately familiar with the study site (unlikely, for this particular site) and/or the methods used, to skim or skip the Methods section, read the Results and Discussion, and return to the methodological details to resolve specific questions that arise. We did reduce redundancy as suggested and feel the Methods section is of reasonable length in its revised form.

In the Results and Discussion, the points raised were consistent with other reviewers and involved critical limitations that must be emphasized. Pia's review helped us identify where and how we should strengthen our discussions around the exploratory/limiting aspects of the study. We believe the discussion of limitations is even more robust after revisions.

Saia, SM, NG Nelson, AS Huseeth, K Grieger, and BJ Reich. 2020. Transitioning Machine Learning from Theory to Practice in Natural Resources Management. *Ecological Modelling* 435: 109257. <https://doi.org/10.1016/j.ecolmodel.2020.109257>.

### **Reviewer 2, Pia Ebeling**

This study uses an interesting innovative approach to estimate transport rates and lag time of NO<sub>3</sub> in the unsaturated and saturated zone from groundwater NO<sub>3</sub> data using random forests. However, the manuscript could be better streamlined according to the messages; especially the method chapter is quite lengthy, repetitive and hard to understand (it is longer than results and discussion). This unfortunately also hampers a clear understanding of the results and discussion chapter in some parts. Some concrete suggestions are given in the detailed comments, though they are not complete and the

method sections needs to be revised. The framework is promising and could replace expensive isotope sampling, therefore, I suggest publication after including the requested changes.

#### Major concerns

Why do you use only vertical velocities? For the unsaturated zone, this concept is common, but I am uncertain why this is used for the saturated zone as well. I did not understand the assumption of shallow groundwater in this context (L.253). Please, clarify this more. Why would it be important to know travel times in vertical dimension without horizontal component? How can the flow be dominantly vertical if the aquifer bottom is considered a no-flow boundary? I think this limitation should also be discussed in the discussion.

AR: This is an important concept, for which we added some text in the Methods (Section 2.4, Lines 214-224). As in many other surficial (water-table) aquifers, we assume groundwater flow is largely horizontal, but with a consistently downward component, such that ground water ages (travel times since recharge) increase with depth. Acknowledging the study area does not represent an idealized surficial aquifer, we listed some general and local observations leading to the linear approximation of vertical groundwater age gradients in this setting. Nonetheless, we certainly agree there is substantial variability in the vertical velocities, which may have limited the performance of the simplified models.

Why do you use the importance of the total travel time to infer transport rates? This argument is not clear for me.

AR: The most direct answer is in the text (lines 303-305): "Total travel time also had the greatest variability in importance among the fifteen variables, with a range of 18.4% between the upper and lower values, suggesting some model sensitivity to lag times."

#### Abstract:

L 17: I do not understand this sentence, though I think I know what you mean. Consider reformulation.

AR: We deleted the word "contrasting" to improve the flow of the sentence.

#### Introduction:

L. 38-39 I do not understand this sentence. What do you mean by "responses ... can be complicated by uncertainties"? Do you mean predictions of responses?

AR: We added the word "Predicting..." to the beginning of the sentence. Thank you for pointing this out.

L 48 Are lag times the same as groundwater ages for you?

AR: No. This sentence refers to both groundwater age-dating (i.e., saturated zone travel time) and vadose zone methods to quantify lag time. Edits for clarification were made in lines 47-48.

L 60-61. Why is the screen depth a proxy for lag times? Wouldn't this only be the case for homogeneous settings and only for vertical movement?

AR: We are referring in this specific sentence to previous studies that used well depth as a proxy for lag times. Observations of vertically stratified groundwater age (increasing age with depth) and nitrate concentrations in aquifers are very common in literature. Hydrologic theory suggests and age-dating studies have shown a strong vertical component to groundwater flow in the shallow parts of the groundwater system. In terms of groundwater age, that is manifested by a linear increase in groundwater age with depth below the water table. We acknowledge that deeper portions of the aquifer may have a greater horizontal component to flow (see additional discussion to comments about horizontal flow below).

Methods (74-290):

**AR overview on Methods section:** Our philosophy on Methods sections is that a reader who is already very familiar with the study site or well-versed in the methods can easily skip to the Results and Discussion section and return later to review methods if questions arise. As recently argued in Saia et al. (2020), machine learning papers warrant more descriptive methodology sections.

Section 2.1 reads very long-winded and not all detail is needed later in the discussion. Please, consider condensing this section.

AR: We appreciate the concern about brevity. However, this section has already been expanded with details in part based on previous reviewers' comments. Further, we feel the site description adds valuable context to the study.

L 114 What are nested wells? Wells with more than one screen?

AR: Yes, as described in Lines 112-119. There is one borehole with multiple tubes, with each tube having the screens at different depths.

Section 2.2 and 2.3: In my opinion, these two sections read quite unfocused and I think they could be condensed and merged into one section. E.g. L. 183-187 This seems unnecessary to explain as this is the principle of random forest which can be easily referenced from literature. Similarly, L 187-196 can be shortened into one sentence saying which approach was used to evaluate variable importance. Actually, 2.2. reads as a summary of what will be explained in 2.3-2.5, which is not necessary. I think you can easily remove it.

AR: Section 2.2 and 2.3 (Section 2.5 in the revised manuscript, after reorganization) were slightly modified to reduce redundancies.

L 169: This sentence seems redundant

AR: Section 2.3 (Section 2.5 in the revised manuscript, after re-organizing) was adjusted to remove redundancies created by this sentence.

L 170 Why did you use nested resampling? I do not see that you discuss those results later. If you used it for tuning, please specify this including the tuning method and parameters.

AR: We used five-repeated five-fold cross-validation to evaluate model performance sensitivity. The five repetitions were performed to account for variation in the data assigned to training/testing splits. To clarify this in the manuscript, the sentence was changed from "This process was repeated five times to create a total of 25 models, similar to the approach used by Nelson et al. (2018)." to "We repeated the

five-fold cross validation process five times to create a total of 25 models, similar to the approach used by Nelson et al. (2018), in order to assess sensitivity of model performance to the data assigned to the training and testing folds.”

L 174 I would suggest the authors to be clearer as permutation importance and pdps are not used to evaluate the model performance but to interpret the model results.

AR: Revised to: “Permutation importance, partial dependence and Nash-Sutcliffe Efficiency (NSE) were quantified to evaluate model performance and to interpret results.”

L 174-182 One sentence is enough to say that you use NSE to evaluate model performance.

AR: We deleted the sentence just above equation 1, which was redundant.

L 198 This sentence is vague and not informative. I would even say it is not correct actually. Within one pdp only one variable (x-axis) is varies while for the others mean values are used. Please reformulate or delete. In my opinion, this paragraph can also be shortened.

AR: Referenced sentence has been removed from the manuscript.

L 204-208 Can be merged into one sentence. It is not relevant to know that data were imported and clipped, just that you selected the “wells within the study area with a corresponding depth ...” would be enough.

AR: We removed the comment about importing and clipping data.

L 233: I am sorry, I did not understand how you use the dynamic descriptors. “annual median [NO<sub>3</sub>] was assigned a lagged dynamic value”, what exactly does that mean? And are the dynamic variables also variable in space?

AR: Dynamic variables were not variable in space as applied in this study. We now point this out as a potential future avenue of exploration (second paragraph of Section 3.1, line 311 in revised manuscript) The exact method for lagging dynamic predictors is given in an example (just below Equation 3, next to last paragraph in Section 2.4 in the revised manuscript).

L 267-269 this sentence is unnecessary like it is. You already state before what range of recharge rates you used. Or maybe the second part could be supported with references: what are those realistic mean values and why are they realistic?

AR: We revised to note in the first sentence that the recharge rates obtained varied by a factor of 4. Then deleted the second sentence as suggested.

L 264-280 Could the calculated parameter ranges of the two paragraphs not be easily presented in a table? It would increase the understanding and not read that lengthy. The text could be strongly shortened then.

AR: These paragraphs explain how we arrived at the range of transport rates. Most of the text would need to remain. In that case, the table would either repeat information in the sentences and/or would only contain two sets of values (the range of vadose-zone and the range of saturated-zone transport rates).

L 285-288 Why did you take this assumption? You could also have used various features derived from the dynamic predictors including mean values over several years. Considering the uncertainty in travel time estimates, I think this approach is not well supported. However, it is still slightly unclear to me how you used the dynamic values and linked them to the annual median [NO<sub>3</sub>]. Did you assign one past value to each well and total lag time (for one transport rate combination)? If so, why do you think this is possible if we also have horizontal groundwater movement and the annual median [NO<sub>3</sub>] is not only dependent on vertical travel times at the well location but on vertical travel times somewhere else plus the horizontal travel times. Please, clarify. Maybe a conceptual figure would help to understand how you link dynamic descriptor values to certain wells and corresponding annual median [NO<sub>3</sub>].

AR: These lines are now located at approximately Lines 250-253 of the revised manuscript. We did assign one past value, as you describe (and as described in the text). It is possible that some other methods could yield results (other studies have used decadal nitrate to roughly estimate travel times, as cited in the introduction, Lines 57-66). Regarding horizontal groundwater flow, please see overview discussion in response to Major Concerns, above.

L 289-293 This part is jumping back to RF application. I think the method section should be restructured with the concept of travel times being presented first and then the RF application used to predict the travel times.

AR: We reorganized the methods sections (2.3 through 2.5) as suggested. The RF details are now in Section 2.5.

Results and Discussion (L. 297- 425)

L 299 Which is the “initial model”? I cannot follow. This should be stated more clearly in the methods.

AR: This was clarified using a parenthetical reference “(using both static and dynamic predictors)”.

L 325-335 This paragraph belongs to the methods. Why do you use the variable importance of total travel times to determine the “optimal” transport rates? I struggle to understand why this approach is promising.

AR: We believe this paragraph belongs in the current location. The information presented here naturally follows text describing the initial round of modelling, which was discussed in the previous section to the paragraph in question. As noted in the second sentence of Section 3.2, we noted substantial variation in total travel time %<sub>inc</sub>MSE. We also note in Section 3.3, bullet #3, the opportunities and limitations to this approach. We are aware of, and discuss, the fact that this approach may not be successful for other studies.

L. 338 Do you think these ratios are transferable to other locations? I would expect this to be site specific. This is not clearly stated here, as the statement sounds rather general.

AR: Thank you for pointing this out. We think the general concept of such ratios could be valuable elsewhere, but these values are specific to the study area. We revised the text to indicate this.

L 345 “second analysis”? What was the paragraph before then? This needs to be specified in the methods.

AR: The paragraph above (first paragraph of Section 3.2) describes the “second analysis”. To clarify, we added a parenthetical reference (“(using only static variables”) to this sentence.

L 346 How uncertain do you see those values considering the equifinality within the  $V_s/V_u$  ratios shown in Fig. 6? Is it meaningful to select one model in this case? Are there more ways to constrain the equifinality problem except data of recharge rates?

AR: While equifinality is an issue with many modelling approaches, we felt the quantitative analysis and subsequent results of the single rate and band of recharge rate ratios compared favorably enough with observed rates that it warranted discussion of both. However, we acknowledge there is considerable uncertainty, and thus our call for further testing and the use of other data to compare with ML model outcomes.

L 355. “mean recharge value derived from groundwater ages in intermediate wells (1.22 m/yr,  $n = 13$ ).” Please provide the reference here.

AR: References have been added (approximately line 355 of the revised version)

3.3 Section: What data or prior knowledge would someone need to apply your new approach to estimate lag times? Would you trust to apply the method without having groundwater ages to validate?

AR: Starting with the abstract of the paper, we highlight limitations of the study and the need for corroboration of results “with a robust conceptual model and complementary information such as groundwater age.” Thus, a robust conceptual model is an essential starting point. In Section 3.3, bullet #3, we state “Testing the approach of using  $\%_{inc}MSE$  in other vadose and saturated zones, with substantial comparison to previous transport rate estimates, is warranted.” Thus, we feel groundwater age or some other comparisons are still necessary when using the approach. This is reinforced by Section 3.3 Opportunities and Limitations..., where four out of five bullets include detailed discussion of model limitations, need for further testing at other sites with different recharge and redox patterns, and other data that could potential guide a similar modeling process.

Do you think this method also works in areas with higher denitrification impact where  $NO_3$  is less conservatively transported? Could the approach be hampered if denitrification potential or other subsurface conditions are heterogeneous (e.g. linked to hot spots such as pyrite lenses or hydraulic conductivity)?

AR: In the second bullet of Section 3.3, we broadened the discussion of nitrate extinction depths to include “heterogeneity in denitrification potential”.

Conclusion:

L 440 What do you mean by “comparisons of data-driven analyses with complementary datasets”

AR: Added examples to the text to help clarify. Text now reads “... comparisons of data-driven analyses with complementary datasets and/or modelling (e.g., field-based recharge rate estimates, finite-difference flow model)”

Figures:

L 686: “ $V_s/V_u$ ”

AR: Thank you for catching this typo. It has been fixed.

# 1 **Determination of vadose and saturated-zone nitrate lag times using long-** 2 **term groundwater monitoring data and statistical machine learning**

3 Martin J. Wells<sup>1,3</sup>, Troy E. Gilmore<sup>2,3</sup>, Natalie Nelson<sup>4,5</sup>, Aaron Mittelstet<sup>3</sup>, J.K. Böhlke<sup>6</sup>,

4 <sup>1</sup>currently at Natural Resources Conservation Service, Redmond, OR, 97756, USA

5 <sup>2</sup>Conservation and Survey Division - School of Natural Resources, University of Nebraska, Lincoln, NE, 68583, USA

6 <sup>3</sup>Biological Systems Engineering, University of Nebraska, Lincoln, NE, 68583, USA

7 <sup>4</sup>Biological and Agricultural Engineering, North Carolina State University, Raleigh, NC, 27695, USA

8 <sup>5</sup>Center for Geospatial Analytics, North Carolina State University, Raleigh, NC, 27695, USA

9 <sup>6</sup>U.S. Geological Survey, Reston, VA, 20192, USA

10 *Correspondence to:* Troy E. Gilmore (gilmore@unl.edu)

11 **Abstract.** In this study, we explored the use of statistical machine learning and long-term groundwater nitrate monitoring data to  
12 estimate vadose-zone and saturated-zone lag times in an irrigated alluvial agricultural setting. Unlike most previous statistical  
13 machine learning studies that sought to predict groundwater nitrate concentrations within aquifers, the focus of this study was to  
14 leverage available groundwater nitrate concentrations and other environmental variables to determine mean regional vertical  
15 velocities (transport rates) of water and solutes in the vadose zone and saturated zone (3.50 m/year and 3.75 m/year, respectively).  
16 The statistical machine learning results are consistent with two **contrasting** primary recharge processes in this Western Nebraska  
17 aquifer: (1) diffuse recharge from irrigation and precipitation across the landscape, and (2) focused recharge from leaking irrigation  
18 conveyance canals. The vadose-zone mean velocity yielded a mean recharge rate (0.46 m/year) consistent with previous estimates  
19 from groundwater age-dating in shallow wells (0.38 m/year). The saturated zone mean velocity yielded a recharge rate (1.31  
20 m/year) that was more consistent with focused recharge from leaky irrigation canals, as indicated by previous results of  
21 groundwater age-dating in intermediate-depth wells (1.22 m/year). Collectively, the statistical machine-learning model results are  
22 consistent with previous observations of relatively high-water fluxes and short transit times for water and nitrate in the primarily  
23 oxic aquifer. Partial dependence plots from the model indicate a sharp threshold where high groundwater nitrate concentrations  
24 are mostly associated with total travel times of seven years or less, possibly reflecting some combination of recent management  
25 practices and a tendency for nitrate concentrations to be higher in diffuse infiltration recharge than in canal leakage water.  
26 Limitations to the machine learning approach include **potential** non-uniqueness of different transport rate combinations when  
27 comparing model performance and highlight the need to corroborate statistical model results with a robust conceptual model and  
28 complementary information such as groundwater age.

29  
30  
31  
32  
33  
34



## 35 1 Introduction

36 Nitrate is a common contaminant of groundwater and surface water that can affect drinking water quality and ecosystem  
37 health. ~~Responses~~ Predicting responses of aquatic resources to changes in nitrate loading can be complicated by uncertainties  
38 related to rates and pathways of nitrate transport from sources to receptors. Lag times for movement of non-point source nitrate  
39 contamination through the subsurface are widely recognized (Böhlke, 2002; Meals et al., 2010; Puckett et al., 2011; Van Meter  
40 and Basu, 2017) but difficult to measure. Vadose (unsaturated zone) and groundwater (saturated zone) lag times are of critical  
41 importance for monitoring, regulating, and managing the transport of contaminants in groundwater. However, transport time-scales  
42 are often generalized due to coarse spatial and temporal resolution in data available for groundwater systems impacted by  
43 agricultural activities (Gilmore et al., 2016; Green et al., 2018; Puckett et al., 2011), resulting in a simplified groundwater  
44 management approach. Regulators and stakeholders in agricultural landscapes are increasingly in need of more precise and local  
45 lag time information to better evaluate and apply regulations and best management practices for the reduction of groundwater  
46 nitrate concentrations (e.g., Eberts et al., 2013).

47 Field-based studies of lag times (time to move through both vadose zone and aquifer) commonly use vadose-zone  
48 sampling and/or expensive groundwater age-dating techniques ~~and/or vadose zone sampling~~ to estimate nitrate transport rates  
49 moving into and through aquifers (Böhlke et al., 2002, 2007; Böhlke and Denver, 1995; Browne and Guldan, 2005; Kennedy et  
50 al., 2009; McMahon et al., 2006; Morgenstern et al., 2015; Turkeltaub et al., 2016; Wells et al., 2018). Detailed process-based  
51 modelling studies focused on lag times require complex numerical models combined with spatially intensive and/or costly  
52 hydrogeological observations (Ilampooranan et al., 2019; Rossman et al., 2014; Russoniello et al., 2016). Thus, efficient but  
53 locally-applicable modelling approaches are needed (Green et al., 2018; Liao et al., 2012; Van Meter and Basu, 2015). In this  
54 study, an alternative data-driven approach (Random Forest Regression) leverages existing long-term groundwater nitrate  
55 concentration (referred to as  $[\text{NO}_3^-]$  hereafter) data and easily accessible environmental data to estimate vadose and saturated-zone  
56 vertical velocities (transport rates) for the determination of subsurface lag times.

57 Statistical machine learning methods, including Random Forest, have been used successfully for modelling  $[\text{NO}_3^-]$   
58 distribution in aquifers (Anning et al., 2012; Juntakut et al., 2019; Knoll et al., 2020; Nolan et al., 2014; Ouedraogo et al., 2017;  
59 Rodriguez-Galiano et al., 2014; Rahmati et al., 2019; Vanclooster et al., 2020; Wheeler et al., 2015), but there has not been robust  
60 analysis of model capabilities for estimating vadose and/or saturated-zone lag times. Proxies for lag time, such as well screen  
61 depth, have been used as predictors in Random Forest models (Nolan et al., 2014; Wheeler et al., 2015). Decadal lag times have  
62 been suggested from using time-averaged nitrogen inputs as predictors (e.g., 1978-1990 inputs vs 1992-2006 inputs) and by  
63 comparing their relative importance in the model (Wheeler et al., 2015). Application of similar machine learning methods  
64 suggested groundwater age could be used as a predictor to improve model performance (Ransom et al., 2017). Hybrid models,  
65 using both mechanistic models and machine learning, have also sought to integrate vertical transport model parameters and outputs  
66 to evaluate nitrate-related predictors, including vadose-zone travel times (Nolan et al., 2018).

67 The objective of this study is to test a data-driven approach for estimating vadose and saturated-zone transport rates and  
68 lag times for an intensively monitored alluvial aquifer in western Nebraska (Böhlke et al., 2007; Verstraeten et al., 2001a, 2001b;  
69 Wells et al., 2018). Results are compared to the hydrogeologic, mechanistic understanding from previous groundwater studies to  
70 determine strengths and weaknesses of the approach as (1) a stand-alone technique, or (2) as an exploratory analysis to guide or  
71 complement more complex physical-based models or intensive hydrogeologic field investigations.

## 72 2 Methods

### 73 2.1 Site Description

74 The Dutch Flats study area is located in the western Nebraska counties of Scotts Bluff and Sioux (Fig. 1). The North  
75 Platte River delivers large quantities of water for crop irrigation in this region and runs along the southern portion of this study  
76 area. Irrigation water is diverted from the North Platte River into three major canals (Mitchell-Gering, Tri-State, and Interstate  
77 Canals) that feed a network of minor canals. Several previous Dutch Flats area studies have investigated groundwater  
78 characteristics and provided thorough site descriptions of the semi-arid region (Babcock et al., 1951; Böhlke et al., 2007;  
79 Verstraeten et al., 2001a, 2001b; Wells et al., 2018). The Dutch Flats area overlies an alluvial aquifer characterized by  
80 unconsolidated deposits of predominantly sand and gravel, with the aquifer base largely consisting of consolidated deposits of the  
81 Brule, Chadron, or Lance Formation (Verstraeten et al., 1995) (Fig. 2). Irrigation water not derived from the North Platte River is  
82 typically pumped from the alluvial aquifer, or water-bearing units of the Brule Formation.

83 The total area of the Dutch Flats study area is roughly 540 km<sup>2</sup>, of which approximately 290 km<sup>2</sup> (53.5%) is agricultural  
84 land (cultivated crops and pasture). Most agricultural land is concentrated south of the Interstate Canal (Homer et al., 2015). Due  
85 to the combination of intense agriculture and low annual precipitation, producers in Dutch Flats rely on a network of irrigation  
86 canals to supply water to the region. From 1908 to 2016, mean precipitation of 390 mm was measured at the nearby Western  
87 Regional Airport in Scottsbluff, NE (NOAA, 2017).

88 While some groundwater is withdrawn for irrigation, and some irrigated acres in the study area are classified as  
89 commingled (groundwater and surface water source), Scotts Bluff County irrigation is mostly from surface water sources.  
90 Estimates determined every five years suggest surface water provided between 76.8% to 98.6% of the total water withdrawals from  
91 1985 to 2015, or about 92% on average (Dieter et al., 2018). Canals transport water from the North Platte River to fields throughout  
92 the study area, most of which are downgradient (south) of the Interstate Canal. Mitchell-Gering, Tri-State, and Interstate Canals  
93 are the major canals in Dutch Flats, with the latter holding the largest water right of 44.5 m<sup>3</sup>/s (NEDNR, 2009). Leakage from  
94 these canals provides a source of artificial groundwater recharge. Previous studies estimate the leakage potential of canals in the  
95 region results in as much as 40% to 50% of canal water being lost during conveyance (Ball et al., 2006; Harvey and Sibray, 2001;  
96 Hobza and Andersen, 2010; Luckey and Cannia, 2006). Leakage estimates from a downstream section of the Interstate Canal  
97 (extending to the east of the study area; Hobza and Andersen (2010)) suggest fluxes ranging from 0.08 to 0.7 m day<sup>-1</sup> through the  
98 canal bed. Assuming leakage of 0.39 m day<sup>-1</sup> over the Interstate Canal bed area (16.8 m width x 55.5 km length) within Dutch  
99 Flats yields 4.1 x 10<sup>5</sup> m<sup>3</sup> day<sup>-1</sup> of leakage. Applied over an on-average 151-day operation period (USBR, 2018), leakage from  
100 Interstate Canal alone could approach 6.1 x 10<sup>7</sup> m<sup>3</sup> annually, or about 29% of the annual volume of precipitation in the Dutch Flats  
101 area.

102 A 1990s study investigated both spatial and temporal influences from canals in the Dutch Flats area (Verstraeten et al.,  
103 2001a, 2001b), with results later synthesized by Böhlke et al. (2007). Canals were found to dilute groundwater [NO<sub>3</sub><sup>-</sup>] locally with  
104 low-[NO<sub>3</sub><sup>-</sup>] (e.g., [NO<sub>3</sub><sup>-</sup>] < 0.06 mg N L<sup>-1</sup> in 1997) surface water during irrigation season. <sup>3</sup>H/<sup>3</sup>He age-dating was used to determine  
105 apparent groundwater ages and recharge rates. It was noted that wells near canals displayed evidence of high recharge rates  
106 influenced by local canal leakage. Data from wells far from the canals indicated that shallow groundwater was more likely  
107 influenced by local irrigation practices (i.e., furrows in fields), while deeper groundwater was impacted by both localized irrigation  
108 and canal leakage (Böhlke et al., 2007). Shallow groundwater in the Dutch Flats area has hydrogen and oxygen stable isotopic  
109 compositions consistent with surface water sources (i.e., North Platte River and associated canals), indicating that most  
110 groundwater intercepted by the monitoring well network has been affected by surface-water irrigation recharge (Böhlke et al.,  
111 2007; Cherry et al., 2020).

112 The Dutch Flats area is within the North Platte Natural Resources District (NPNRD), one of 23 groundwater management  
113 districts in Nebraska tasked with, among other functions, improving water quality and quantity. The NPNRD has a large monitoring  
114 well network consisting of 797 wells, 327 of which are nested. Nested well clusters are drilled and constructed such that screen  
115 intervals represent (1) “shallow” groundwater intersecting the water table (length of screened interval = 6.1 m), (2) “intermediate”  
116 groundwater from mid-aquifer depths (length of screened interval = 1.5 m), and “deep” groundwater near the base of the unconfined  
117 aquifer (length of screened interval = 1.5 m). Depending on well location within the Dutch Flats area, depths of the water table and  
118 base of aquifer are highly variable, such that shallow, intermediate, and deep wells can have overlapping ranges of depths below  
119 land surface (Fig. 2).

120 Influenced by both regulatory and economic incentives, the Dutch Flats area has undergone a notable shift in irrigation  
121 practices in the last two decades. From 1999 to 2017, center pivot irrigated area has increased by approximately 270%, from  
122 roughly 3,830 hectares to 14,253 hectares, or from 13% to 49% of the total agricultural land area, respectively. [The majority of Most](#)  
123 [of this shift in technology has occurred on fields previously under furrow irrigation.](#) Conventional furrow irrigation has an estimated  
124 potential application efficiency (“measure of the fraction of the total volume of water delivered to the farm or field to that which  
125 is stored in the root zone to meet the crop evapotranspiration needs,” per Irmak et al. (2011)) of 45% to 65%, compared to center  
126 pivot sprinklers at 75% to 85% (Irmak et al., 2011). Based on improved irrigation efficiency (between 10-40%), average  
127 precipitation throughout growing season (29.5 cm for 15 April to 13 October (Yonts, 2002)), and average water requirements for  
128 corn (69.2 cm (Yonts, 2002)), converting furrow irrigated fields to center pivot over the aforementioned 14,253 hectares could  
129 represent a difference of  $1 \times 10^7 \text{ m}^3$  to  $6 \times 10^7 \text{ m}^3$  in water applied. Those (roughly approximated) differences in water volumes are  
130 equivalent to 6% to 28% of average annual precipitation applied over the Dutch Flats area, suggesting the change in irrigation  
131 practice does have potential to alter the water balance in the area.

132 The hypothesis of lower recharge due to changes in irrigation technology was investigated by Wells et al. (2018) by  
133 comparing samples collected in 1998 and 2016. Sample sites were selected based on a well’s proximity to fields that observed a  
134 conversion in irrigation practices (i.e., furrow irrigation to center pivot) between the two collection periods. While mean recharge  
135 rate was not significantly different, a lower recharge rate was indicated by data from 88% of the wells. Long-term Dutch Flats  
136  $[\text{NO}_3^-]$  trends were also assessed in the study, suggesting decreasing trends (though statistically insignificant) from 1998 to 2016  
137 throughout the Dutch Flats area, and nitrogen isotopes of nitrate indicated little change in biogeochemical processes. For additional  
138 background, Wells et al., (2018) provides a more in-depth analysis of recent  $[\text{NO}_3^-]$  trends in this region (see also, Fig. S1A [in the](#)  
139 [online Supplemental Material](#), which shows the nitrate data used in the present study).

140 As in other agricultural areas, nitrate in Dutch Flats groundwater is dependent on nitrogen loading at the land surface, rate  
141 of leaching below crop root zones, rate of nitrate transport through the vadose and saturated zones, dilution from focused recharge  
142 in the vicinity of canals, rate of discharge from the aquifer (whether from pumping or discharge to surface water bodies), and rates  
143 of nitrate reduction (primarily denitrification) in the aquifer. Based on nitrogen and oxygen isotopes in nitrate and redox conditions  
144 observed in previous studies, denitrification likely has a relatively minor or localized influence on groundwater nitrate in the Dutch  
145 Flats area (Wells et al., 2018). Evidence of denitrification (from dissolved gases and isotopes (Böhlke et al., 2007, Wells et al.  
146 2018)) was mostly limited to some of the deepest wells near the bottom of the aquifer. Leakage of low-nitrate water in the major  
147 canals causes nitrate dilution in the groundwater (i.e., relatively little nitrate addition, at least from the upgradient canals).  
148 Additional isotope data might be useful for documenting temporal shifts in recharge sources, or irrigation return flows to the river;  
149 however, it is difficult to know exactly the location or size of the contributing area for each well, especially the deeper ones.

150 Other long-term changes to the landscape were evaluated by Wells et al. (2018) and included statistically significant  
151 reductions in mean fertilizer application rates (1987–1999 vs. 2000–2012) and volume of water diverted into the Interstate Canal

152 (1983–1999 vs. 2000–2016), while a significant increase in area of planted corn occurred (1983–1999 vs. 2000–2016).  
153 Precipitation was also evaluated, and though the mean has decreased over a similar time period, the trend was not statistically  
154 significant.

## 155 2.2 Statistical Machine Learning Modelling Framework

156 Statistical machine learning uses algorithms to assess and identify complex relationships between variables. Learned  
157 relations can be used to uncover nonlinear trends in data that might otherwise be overshadowed when using simple regression  
158 techniques (Hastie et al., 2009). In this study we used Random Forest Regression, ~~where Random Forests are created by combining~~  
159 ~~hundreds of unskilled regression trees into one model ensemble, or “forest”, which collectively produce skilled and robust~~  
160 ~~predictions (Breiman, 2001). Predictors used in the model represent~~ to evaluate site-specific explanatory variables (e.g.,  
161 precipitation, vadose-zone thickness, depth to bottom of screen, etc.) that may impact the response variable, groundwater [NO<sub>3</sub>].  
162 Additionally, as described in detail in Section 2.5.4, we estimated a range of total travel times (from land surface to the point of  
163 sampling) at each of the wells by varying vadose and saturated-zone transport rates. The relative importance of total travel time as  
164 a predictor variable was ultimately used to identify an optimal travel time and model.

## 165 2.3 Variables and Project Setup

166 Data from 15 predictors were collected and analysed (Table 1). Spatial variables were manipulated using ArcGIS 10.4.  
167 The [NO<sub>3</sub>]<sup>-</sup> dataset for the entire NPNRD had 10,676 observations from 1979 to 2014, and was downloaded from the Quality-  
168 Assessed Agrichemical Contaminant Database for Nebraska Groundwater (University of Nebraska-Lincoln, 2016). We used data  
169 encompassed by the Dutch Flats model area (2,829 [NO<sub>3</sub>]<sup>-</sup> observations from 214 wells). In order to have an accurate vadose-zone  
170 thickness, only wells with a corresponding depth to groundwater record, of which the most recent record was used, were selected  
171 (2,651 observations from 172 wells). Over this period, several wells were sampled much more frequently than others (e.g., monthly  
172 sampling, over a short period of record), especially during a U.S. Geological Survey (USGS) National Water-Quality Assessment  
173 (NAWQA) study from 1995 to 1999. To prevent those wells from dominating the training and testing of the model, annual median  
174 [NO<sub>3</sub>]<sup>-</sup> was calculated for each well and used in the dataset. The dataset was further manipulated such that each median [NO<sub>3</sub>]<sup>-</sup>  
175 observation had 15 complementary predictors (Table 1). The selected predictor variables capture drivers of long-term [NO<sub>3</sub>]<sup>-</sup> and  
176 [NO<sub>3</sub>]<sup>-</sup> lags. After incorporating all data, including limited records of dissolved oxygen (DO), the final dataset included 1,049  
177 [NO<sub>3</sub>]<sup>-</sup> observations from 162 wells sampled between 1993 and 2013 (Figure S1A). Additional details of the data selection, sources,  
178 and manipulations may be found in the Supplemental Material.

179 Predictors were divided into two categories: static and dynamic (Table 1). Static predictors are those that either do not  
180 change over the period of record, or annual records were limited. DO, for example, could potentially experience slight annual  
181 variations, but data were not available to assign each nitrate sample a unique DO value. Instead, observations for each well were  
182 assigned the average DO value observed from the well. This approximation was considered reasonable because nitrate isotopic  
183 composition and DO data collected in the 1990s and by Wells et al. (2018) did not indicate any major changes to biogeochemical  
184 processes over nearly two decades. Total travel time (from ground surface to the point of sampling) was strictly considered a static  
185 predictor in this study and was used to link the nitrate-sampling year to a dynamic predictor value.

186 Dynamic predictors were defined in this study as data that changed temporally over the study period. Therefore, each  
187 annual median [NO<sub>3</sub>]<sup>-</sup> was assigned a lagged dynamic value to represent the difference between the time of a particular surface  
188 activity (e.g., timing of a particular irrigation practice) and when groundwater sampling occurred. Dynamic predictors were  
189 available from 1946 to 2013 and included annual precipitation, Interstate Canal discharge, area under center pivot sprinklers, and

190 area of planted corn (Fig. 3). Dynamic predictors were included to assess their ability to optimize Random Forest groundwater  
191 modelling and determine an appropriate lag time. Lag times were based on the vertical travel distance through both the vadose and  
192 saturated zones (see Section 2.4). Area of planted corn was included as a proxy for fertilizer data, which were unavailable prior to  
193 1987. However, analysis suggests there has been a 17% reduction (comparing the means of 1987-1999 to 2000-2012) in fertilizer  
194 application rates per planted hectare, while area of planted corn has increased 16% (comparing the means of 1983-1999 to 2000-  
195 2016) in recent decades (Wells et al., 2018). This trend may be attributed to improved fertilizer management by agricultural  
196 producers. There was a likely trade-off in using this proxy; we were able to extend the period of record back to 1946, allowing for  
197 analysis of a wider range of lag times in the model, but might have sacrificed some accuracy in recent decades when nitrogen  
198 management may have improved. Lastly, vadose and saturated-zone transport rates were assumed to be constant over time (Wells  
199 et al., 2018).

#### 200 **2.4 Vadose and Saturated-zone Transport Rate Analysis**

201 Ranges of vertical velocities (transport rates) through the Dutch Flats vadose zone and saturated zone were estimated  
202 from  $^3\text{H}/^3\text{He}$  age-dating derived recharge rates. The vertical velocities were determined from results published for samples collected  
203 in 1998 (Böhlke et al., 2007, Verstraeten et al., 2001a) and 2016 (Wells et al., 2018) as

$$204 V = \frac{R}{\theta} \quad (1)$$

205 where  $R$  is the upper and lower bound of recharge rates (m/yr), and  $\theta$  is the mobile water content in the vadose zone or porosity in  
206 the saturated zone. The  $^3\text{H}/^3\text{He}$  data were used in this study solely for constraining the range of potential transport rates to evaluate  
207 in the vadose and saturated zones, and as a base comparison to model results. The age-data, however, were not used by the model  
208 itself when seeking to identify an optimum transport rate combination. Throughout the text, unsaturated (vadose)-zone vertical  
209 transport rates will be abbreviated as  $V_u$ , while saturated-zone vertical transport rates will be  $V_s$ . In the vadose zone,  $\theta$  was assigned  
210 a constant value of 0.13, which was calibrated previously using a vertical transport model for the Dutch Flats area (Liao et al.,  
211 2012). In the saturated zone,  $\theta$  was assigned a constant value of 0.35, equal to the value assumed previously for recharge  
212 calculations (Böhlke et al., 2007). Vadose and saturated-zone travel times ( $\tau$ ) then were calculated using Equation 2:

$$213 \tau = \frac{z}{v} \quad (2)$$

214 where  $\tau$  is either vadose zone ( $\tau_u$ ) or saturated zone ( $\tau_s$ ) travel time in years, and  $z$  is the vadose-zone thickness ( $z_u$ ) or distance  
215 from the water table to well mid-screen ( $z_s$ ) in meters.

216 Though Equations 21 and 32 do not explicitly consider horizontal groundwater flow, they are approximately consistent  
217 with the distribution of groundwater ages (travel times from recharge), which increase with depth below the water table. Whereas  
218 groundwater ages commonly increase exponentially with depth in idealized surficial aquifers with relatively uniform thickness and  
219 distributed recharge (Cook and Böhlke, 2000), our linear approximation is based on several local observations, including (1) the  
220 linear approximation is similar to the exponential approximation in the upper parts of idealized aquifers; (2) linear age gradients  
221 may be appropriate in idealized wedge-shaped flow systems, as in some segments of the aquifer section (Figure 2); and (3) focused  
222 recharge under irrigation canals and distribution channels can cause distortion of vertical groundwater age gradients in  
223 downgradient parts of the flow system; and (4) roughly linear age gradients were obtained from groundwater dating in the region,  
224 though with substantial local variability (Böhlke et al., 2007), believed to adequately model shallow groundwater ages, which are  
225 likely to follow approximately linear vertical age gradients near the water table. These simple equations are also suggested to  
226 sufficiently estimate groundwater age gradients in wedge-shaped aquifers (Cook and Böhlke, 2000), and Böhlke et al. (2007) found  
227 a linear model adequately fit their data in the Dutch Flats area. Discrete transport rates and travel times calculated from Equations 21

Formatted: Not Highlight

228 and 32 should be considered “apparent” rates and travel times, similar to apparent groundwater ages, which are based on imperfect  
229 tracers and may be affected by dispersion and mixing. Nonetheless, the saturated open intervals of the monitoring wells used for  
230 this study (< 6.1 m for shallow wells; 1.5 m for intermediate and deep wells) generally were short compared with the aquifer  
231 thickness, such that age distributions within individual samples were relatively restricted in comparison to those of the whole  
232 aquifer or of wells with long screened intervals. Additionally, it is emphasized that the assumed mobile water  
233 content of 0.13 is a calibrated parameter derived previously through inverse modelling and, as suggested by Liao et al. (2012), may  
234 have large uncertainties due to the varying site-specific characteristics known to exist from one well to the next.

235 Because of the influence of canal leakage on both intermediate and deep wells (Böhlke et al., 2007), only recharge rates  
236 from shallow wells were used to estimate initial values and permissible ranges of vadose-zone travel times. The mean ( $\bar{x} = 0.38$   
237 m/yr) and standard deviation ( $\sigma = \pm 0.23$  m/yr) of all the 1998 (n = 7) and 2016 (n = 2) shallow recharge rates were calculated.  
238 Using  $\bar{x} \pm 1\sigma$ , a range of recharge rates from 0.15 to 0.61 m/yr (i.e., rates that varied by a factor of four) were converted to transport  
239 rates ( $V_v$ ) using Equation 1. Calculated transport rates resulted in 1.15 to 4.69 m/yr as the range of vadose-zone transport rates.  
240 Expanding the upper and lower bounds, a minimum vadose-zone transport rate of 1.0 m/yr and maximum of 4.75 m/yr was applied.  
241 Vertical transport rates in the vadose zone were increased by increments of 0.25 m/yr from 1.0 to 4.75 m/yr, resulting in 16 possible  
242 vadose-zone transport rates to evaluate in the Random Forest model.

243 Mean ( $\bar{x} = 0.84$  m/yr) and standard deviation ( $\sigma = \pm 0.73$  m/yr) of all shallow, intermediate, and deep well recharge rates  
244 were included in identifying a range of saturated-zone recharge rates from 0.10 to 1.57 m/yr. A total of 35 and 8 recharge rates  
245 were used from the Böhlke et al. (2007) and Wells et al. (2018) studies, respectively. Equation 1 was used to calculate saturated-  
246 zone transport rates ( $V_s$ ) of 0.28 and 4.49 m/yr. Saturated-zone transport rates were increased by increments of 0.25 m/yr, from  
247 0.25 to 4.5 m/yr, resulting in 18 unique saturated-zone transport rates to evaluate in the Random Forest model. The range of  
248 transport rates suggested by groundwater age-dating was large (more than an order of magnitude) and are considered to include  
249 rates likely to be expected in a variety of field settings. Presumably, similar model constraints and results could have been obtained  
250 without the prior age data and with some relatively conservative estimates.

251 Travel times  $\tau_u$  and  $\tau_s$  were calculated for each well based on  $z_u$  and  $z_s$ , respectively. For every possible combination of  
252 vadose and saturated-zone transport rates, a unique total travel time,  $\tau_t$ , was calculated for each well based on the vadose and  
253 saturated-zone dimensions of that particular well.

$$254 \tau_t = \tau_u + \tau_s \quad (3)$$

255 The total travel times from Equation 3 were used to lag dynamic predictors relative to each nitrate sample date. For  
256 instance, a nitrate sample collected in 2010 at a well with a 20-year total travel time (e.g.,  $\tau_u = 10$  yrs and  $\tau_s = 10$  yrs) would be  
257 assigned the 1990 values for precipitation (450 mm), Interstate Canal discharge (0.4 km<sup>3</sup>/yr), center pivot irrigated area (2484  
258 hectares), and area of planted corn (8905 hectares).

259 A total of 288 unique transport rate combinations (corresponding to different combinations of the 16 vadose and 18  
260 saturated-zone transport rates) were evaluated. Each transport rate combination incorporated up to 1,049 groundwater [NO<sub>3</sub><sup>-</sup>] values  
261 in the Random Forest model.

## 262 **2.5 Random Forest Application**

263 Random Forests are created by combining hundreds of unskilled regression trees into one model ensemble, or “forest”,  
264 which collectively produce skilled and robust predictions (Breiman, 2001). Models of groundwater [NO<sub>3</sub><sup>-</sup>] were developed using  
265 five-fold cross validation (Hastie et al., 2009), where each fold was used to build the model (training data) four times, and held out  
266 once (testing data). The maximum and minimum of the groundwater [NO<sub>3</sub><sup>-</sup>] and each predictor were determined and placed into

267 each fold for training models to eliminate the potential for extrapolation during validation. The four folds designated to build the  
268 model also underwent a nested five-fold cross validation, as specified in the *trainControl* function within the *caret* (Classification  
269 and Regression Training) R package (Kuhn, 2008; R Core Team, 2017). Functions in *caret* were used to train the Random Forest  
270 models. We repeated the five-fold cross validation process five times to create a total of 25 models, similar to the approach used  
271 by Nelson et al. (2018), in order to assess sensitivity of model performance to the data assigned to the training and testing folds.

272 Permutation importance, partial dependence and Nash-Sutcliffe Efficiency (NSE)) were quantified to evaluate model  
273 performance and to interpret results. NSE (Nash and Sutcliffe, 1970) was calculated as

$$274 \text{NSE} = 1 - \frac{\sum_{i=1}^n (Y_i^{\text{obs}} - Y_i^{\text{pred}})^2}{\sum_{i=1}^n (Y_i^{\text{obs}} - Y^{\text{mean}})^2} \quad (4)$$

275 where  $n$  is the number of observations,  $Y_i^{\text{obs}}$  is the  $i^{\text{th}}$  observation of the response variable ( $[\text{NO}_3^-]$ ),  $Y_i^{\text{pred}}$  is the  $i^{\text{th}}$  prediction from  
276 the Random Forest model, and  $Y^{\text{mean}}$  is the mean of observations  $i$  through  $n$ . Values from negative infinity to 0 suggest the mean  
277 of the observed  $[\text{NO}_3^-]$  would serve as a better predictor than the model. When  $\text{NSE} = 0$ , model predictions are as accurate as that  
278 of a model with only the mean observed  $[\text{NO}_3^-]$  as a predictor. From 0, larger NSE values indicate a model's predictive ability  
279 improves, until  $\text{NSE} = 1$ , where observations and predictions are equal. NSE was calculated for both the training and testing data.

280 For each tree, a random bootstrapped sample (i.e., data randomly pulled from the dataset, sampled with replacement) is  
281 extracted from the dataset (Efron, 1979), as well as a random subset of predictors to consider fitting at each split. Thus, each tree  
282 is grown from a bootstrap sample and random subset of predictors, making trees random and grown independent of the others.  
283 Observations not used as bootstrap samples are termed out-of-bag (OOB) data.

284 When building a tree, all  $[\text{NO}_3^-]$  from the bootstrap sample are categorized into terminal nodes, such that each node is  
285 averaged and yields a predicted  $[\text{NO}_3^-]$ . The performance and mean squared error (MSE) of a Random Forest model is evaluated  
286 by comparing the observed  $[\text{NO}_3^-]$  of the OOB data to the average predicted  $[\text{NO}_3^-]$  from the forest. OOB data from the training  
287 dataset may be used to evaluate both permutation importance, referred to in the rest of this text as variable importance, and partial  
288 dependence. Variable importance uses percent increase in mean squared error ( $\%_{\text{incMSE}}$ ) to describe predictive power of each  
289 predictor in the model (Jones and Linder, 2015). During this process, a single predictor is permuted, or shuffled, in the dataset.  
290 Therefore, each observed  $[\text{NO}_3^-]$  has the same relationship between itself and all predictors, except one permuted variable. The  
291  $\%_{\text{incMSE}}$  of a variable is determined by comparing the permuted OOB MSE to unpermuted OOB MSE. Important predictors will  
292 result in a large  $\%_{\text{incMSE}}$ , while a variable of minor importance does little to impact a model's performance, as suggested by a low  
293  $\%_{\text{incMSE}}$  value.

294 Partial dependence curves serve as a graphical representation of the relationship between  $[\text{NO}_3^-]$  and predictors in the  
295 Random Forest model ensemble (Hastie et al., 2009). In these models, the y-axis of a partial dependence plot represents the average  
296 of the OOB predicted  $[\text{NO}_3^-]$  at a specific x-value of each predictor.

297 Random Forests are created by combining hundreds of unskilled regression trees into one model ensemble, or "forest",  
298 which collectively produce skilled and robust predictions (Breiman, 2001). Random Forest regression models of groundwater  
299  $[\text{NO}_3^-]$  were developed using five-fold cross validation (Hastie et al., 2009), where each fold was used to build the model (training  
300 data) four times, and held out once (testing data). The maximum and minimum of the groundwater  $[\text{NO}_3^-]$  and each predictor were  
301 determined and placed into each fold for training models to eliminate the potential for extrapolation during validation. The four  
302 folds designated to build the model also underwent a nested five-fold cross validation, as specified in the *trainControl* function  
303 within the *caret* (Classification and Regression Training) R package (Kuhn, 2008; R Core Team, 2017). Functions in *caret* were  
304 used to train the Random Forest models.

Formatted: Normal, Indent: First line: 0.5"

305 where four folds were used to build the model (training data), and one fold was held out (testing data). The maximum and  
306 minimum of the  $[\text{NO}_2^-]$  and each predictor were determined and placed into each fold for training models to eliminate the potential  
307 for extrapolation during validation. Each fold was used as training data four times, and testing data once. This process was repeated  
308 five times to create a total of 25 models, similar to the approach used by Nelson et al. (2018). ~~The four folds designated to build~~  
309 ~~the model underwent a nested five-fold cross validation, as specified in the *trainControl* function within the *caret* (Classification~~  
310 ~~and Regression Training) R package (Kuhn, 2008; R Core Team, 2017). Functions in *caret* were used to train the Random Forest~~  
311 ~~models. We repeated the five-fold cross validation process five times to create a total of 25 models, similar to the approach used~~  
312 ~~by Nelson et al. (2018), in order to assess sensitivity of model performance to the data assigned to the training and testing folds.~~

313  
314 To evaluate model performance, Nash-Sutcliffe Efficiency (NSE), permutation importance, and partial dependence were  
315 quantified. NSE indicates the degree to which observed and predicted values deviate from a 1:1 line, and ranges from negative  
316 infinity to 1 (Nash and Sutcliffe, 1970).

$$317 \quad NSE = 1 - \frac{\sum_{i=1}^n (Y_i^{obs} - Y_i^{pred})^2}{\sum_{i=1}^n (Y_i^{obs} - \bar{Y}^{mean})^2}, \quad (1)$$

318 where  $n$  is the number of observations,  $Y_i^{obs}$  is the  $i^{\text{th}}$  observation of the response variable ( $[\text{NO}_2^-]$ ),  $Y_i^{pred}$  is the  $i^{\text{th}}$   
319 prediction from the Random Forest model, and  $\bar{Y}^{mean}$  is the mean of observations  $i$  through  $n$ . Values from negative infinity to 0  
320 suggest the mean of the observed  $[\text{NO}_2^-]$  would serve as a better predictor than the model. When  $NSE = 0$ , model predictions are  
321 as accurate as that of a model with only the mean observed  $[\text{NO}_2^-]$  as a predictor. From 0, larger NSE values indicate a model's  
322 predictive ability improves, until  $NSE = 1$ , where observations and predictions are equal. NSE was calculated for both the training  
323 and testing data.

324 For each tree, a random bootstrapped sample (i.e., data randomly pulled from the dataset, sampled with replacement) is  
325 extracted from the dataset (Efron, 1979), as well as a random subset of predictors to consider fitting at each split. Thus, each tree  
326 is grown from a bootstrap sample and random subset of predictors, making trees random and grown independent of the others.  
327 Observations not used as bootstrap samples are termed out-of-bag (OOB) data.

328 When building a tree, all  $[\text{NO}_2^-]$  from the bootstrap sample are categorized into terminal nodes, such that each node is  
329 averaged and yields a predicted  $[\text{NO}_2^-]$ . The performance and mean squared error (MSE) of a Random Forest model is evaluated  
330 by comparing the observed  $[\text{NO}_2^-]$  of the OOB data to the average predicted  $[\text{NO}_2^-]$  from the forest. OOB data from the training  
331 dataset may be used to evaluate both permutation importance, referred to in the rest of this text as variable importance, and partial  
332 dependence. Variable importance uses percent increase in mean squared error ( $\%_{\text{incMSE}}$ ) to describe predictive power of each  
333 predictor in the model (Jones and Linder, 2015). During this process, a single predictor is permuted, or shuffled, in the dataset.  
334 Therefore, each observed  $[\text{NO}_2^-]$  has the same relationship between itself and all predictors, except one permuted variable. The  
335  $\%_{\text{incMSE}}$  of a variable is determined by comparing the permuted OOB MSE to unpermuted OOB MSE. Important predictors will  
336 result in a large  $\%_{\text{incMSE}}$ , while a variable of minor importance does little to impact a model's performance, as suggested by a low  
337  $\%_{\text{incMSE}}$  value.

338 Partial dependence curves serve as a graphical representation of the relationship between  $[\text{NO}_2^-]$  and predictors in the  
339 Random Forest model ensemble (Hastie et al., 2009). Each plot considers the effects of other variables in the model, because  
340 predictions of  $[\text{NO}_2^-]$  are influenced by several predictors when building each tree. In these models, the y-axis of a partial  
341 dependence plot represents the average of the OOB predicted  $[\text{NO}_2^-]$  at a specific x-value of each predictor.

#### 342 2.4 Variables and Project Setup

Formatted: Indent: First line: 0.5"

Formatted: Normal, Indent: First line: 0.5"



343 Data from 15 predictors were collected and analysed (Table 1). Spatial variables were manipulated using ArcGIS 10.4.  
344 The [NO<sub>3</sub><sup>-</sup>] dataset for the entire NPNRD had 10,676 observations from 1979 to 2014, and was downloaded from the Quality-  
345 Assessed Agrichemical Contaminant Database for Nebraska Groundwater (University of Nebraska-Lincoln, 2016). Spatial  
346 locations for each well were included in the original [NO<sub>3</sub><sup>-</sup>] dataset and imported into GIS. Wells were clipped to the Dutch Flats  
347 model area, resulting in 2,829 [NO<sub>3</sub><sup>-</sup>] observations from 214 wells. In order to have an accurate vadose zone thickness, only wells  
348 with a corresponding depth to groundwater record, of which the most recent record was used, were selected (2,651 observations  
349 from 172 wells). Over this period, several wells were sampled much more frequently than others (e.g., monthly sampling, over a  
350 short period of record), especially during a U.S. Geological Survey (USGS) National Water Quality Assessment (NAWQA) study  
351 from 1995 to 1999. In order to prevent those wells from dominating the training and testing of the model, annual median [NO<sub>3</sub><sup>-</sup>]  
352 ] was calculated for each well and used in the dataset. The dataset was further manipulated such that each median [NO<sub>3</sub><sup>-</sup>]  
353 observation had 15 complementary predictors (Table 1). The selected predictor variables capture drivers of long-term [NO<sub>3</sub><sup>-</sup>] and  
354 [NO<sub>3</sub><sup>-</sup>] lags. After incorporating all data, including limited records of dissolved oxygen (DO), the final dataset included 1,049  
355 [NO<sub>3</sub><sup>-</sup>] observations from 162 wells sampled between 1993 and 2013 (Figure S1A). Additional details of the data selection, sources,  
356 and manipulations may be found in the supplemental material.

357 Predictors were divided into two categories: static and dynamic (Table 1). Static predictors are those that either do not  
358 change over the period of record, or annual records were limited. DO, for example, could potentially experience slight annual  
359 variations, but data were not available to assign each nitrate sample a unique DO value. Instead, observations for each well were  
360 assigned the average DO value observed from the well. This approximation was considered reasonable because nitrate isotopic  
361 composition and DO data collected in the 1990s and by Wells et al. (2018) did not indicate any major changes to biogeochemical  
362 processes over nearly two decades. Total travel time (from ground surface to the point of sampling) was strictly considered a static  
363 predictor in this study and was used to link the nitrate sampling year to a dynamic predictor value.

364 Dynamic predictors were defined in this study as data that changed temporally over the study period. Therefore, each  
365 annual median [NO<sub>3</sub><sup>-</sup>] was assigned a lagged dynamic value to represent the difference between the time of a particular surface  
366 activity (e.g., timing of a particular irrigation practice) and when groundwater sampling occurred. Dynamic predictors were  
367 available from 1946 to 2013 and included annual precipitation, Interstate Canal discharge, area under center pivot sprinklers, and  
368 area of planted corn (Fig. 3). Dynamic predictors were included to assess their ability to optimize Random Forest groundwater  
369 modelling and determine an appropriate lag time. Lag times were based on the vertical travel distance through both the vadose and  
370 saturated zones (see Section 2.5). Area of planted corn was included as a proxy for fertilizer data, which were unavailable prior to  
371 1987. However, analysis suggests there has been a 17% reduction (comparing the means of 1987–1999 to 2000–2012) in fertilizer  
372 application rates per planted hectare, while area of planted corn has increased 16% (comparing the means of 1983–1999 to 2000–  
373 2016) in recent decades (Wells et al., 2018). This trend may be attributed to improved fertilizer management by agricultural  
374 producers. There was a likely trade-off in using this proxy; we were able to extend the period of record back to 1946, allowing for  
375 analysis of a wider range of lag times in the model, but might have sacrificed some accuracy in recent decades when nitrogen  
376 management may have improved. Lastly, vadose and saturated zone transport rates were assumed to be constant over time (Wells  
377 et al., 2018).

### 378 2.5 Vadose and Saturated zone Transport Rate Analysis

379 Ranges of vertical velocities (transport rates) through the Dutch Flats vadose zone and saturated zone were estimated  
380 from <sup>3</sup>H/<sup>3</sup>He age dating derived recharge rates. The vertical velocities were determined from results published for samples collected  
381 in 1998 (Böhlke et al., 2007; Verstraeten et al., 2001a) and 2016 (Wells et al., 2018) as

$$382 \quad V = \frac{R}{\theta'} \quad (2)$$

Formatted: Normal, Indent: First line: 0.5"

Formatted: Indent: First line: 0.5"

383 where  $R$  is the upper and lower bound of recharge rates (m/yr), and  $\theta$  is the mobile water content in the vadose zone or  
 384 porosity in the saturated zone. The  $^3\text{H}/^3\text{He}$  data were used in this study solely for constraining the range of potential transport  
 385 rates to evaluate in the vadose and saturated zones, and as a base comparison to model results. The age data, however, were not  
 386 used by the model itself when seeking to identify an optimum transport rate combination. Throughout the text, unsaturated  
 387 (vadose) zone vertical transport rates will be abbreviated as  $V_u$ , while saturated zone vertical transport rates will be  $V_s$ . In the  
 388 vadose zone,  $\theta$  was assigned a constant value of 0.13, which was calibrated previously using a vertical transport model for the  
 389 Dutch Flats area (Liao et al., 2012). In the saturated zone,  $\theta$  was assigned a constant value of 0.35, equal to the value assumed  
 390 previously for recharge calculations (Böhlke et al., 2007). Vadose and saturated zone travel times ( $\tau$ ) then were calculated using  
 391 Equation 3:

$$392 \quad \tau = \frac{z}{V}, \quad (3)$$

393 where  $\tau$  is either vadose zone ( $\tau_u$ ) or saturated zone ( $\tau_s$ ) travel time in years, and  $z$  is the vadose zone thickness ( $z_u$ ) or  
 394 distance from the water table to well mid-screen ( $z_s$ ) in meters.

395 Though Equations 2 and 3 do not explicitly consider horizontal groundwater flow, they are believed to adequately model  
 396 shallow groundwater ages, which are likely to follow approximately linear vertical age gradients near the water table. These simple  
 397 equations are also suggested to sufficiently estimate groundwater age gradients in wedge shaped aquifers (Cook and Böhlke, 2000),  
 398 and Böhlke et al. (2007) found a linear model adequately fit their data in the Dutch Flats area. Discrete transport rates and travel  
 399 times calculated from Equations 2 and 3 should be considered “apparent” rates and travel times, similar to apparent groundwater  
 400 ages, which are based on imperfect tracers and may be affected by dispersion and mixing. Nonetheless, the saturated open intervals  
 401 of the monitoring wells used for this study (< 6.1 m for shallow wells; 1.5 m for intermediate and deep wells) generally were short  
 402 compared with the aquifer thickness, such that age distributions of individual samples were relatively restricted in comparison to  
 403 those of the whole aquifer or wells with long screened intervals. Additionally, it is emphasized that the assumed mobile water  
 404 content of 0.13 is a calibrated parameter derived previously through inverse modelling and, as suggested by Liao et al. (2012), may  
 405 have large uncertainties due to the varying site specific characteristics known to exist from one well to the next.

406 Because of the influence of canal leakage on both intermediate and deep wells (Böhlke et al., 2007), only recharge rates  
 407 from shallow wells were used to estimate initial values and permissible ranges of vadose zone travel times. The mean ( $\bar{x} = 0.38$   
 408 m/yr) and standard deviation ( $\sigma = \pm 0.23$  m/yr) of all the 1998 ( $n = 7$ ) and 2016 ( $n = 2$ ) shallow recharge rates were calculated.  
 409 Using  $\bar{x} \pm 1\sigma$ , a range of recharge rates from 0.15 to 0.61 m/yr were converted to transport rates ( $V_u$ ) using Equation 2. One standard  
 410 deviation was selected to constrain the range of rates evaluated, as we considered this method likely encompassed realistic mean  
 411 field values. Calculated transport rates resulted in 1.15 to 4.69 m/yr as the range of vadose zone transport rates. Expanding the  
 412 upper and lower bounds, a minimum vadose zone transport rate of 1.0 m/yr and maximum of 4.75 m/yr was applied. Vertical  
 413 transport rates in the vadose zone were increased by increments of 0.25 m/yr from 1.0 to 4.75 m/yr, resulting in 16 possible vadose-  
 414 zone transport rates to evaluate in the Random Forest model.

415 Mean ( $\bar{x} = 0.84$  m/yr) and standard deviation ( $\sigma = \pm 0.73$  m/yr) of all shallow, intermediate, and deep well recharge rates  
 416 were included in identifying a range of saturated zone recharge rates from 0.10 to 1.57 m/yr. A total of 35 and 8 recharge rates  
 417 were used from the Böhlke et al. (2007) and Wells et al. (2018) studies, respectively. Equation 2 was used to calculate saturated-  
 418 zone transport rates ( $V_s$ ) of 0.28 and 4.49 m/yr. Saturated zone transport rates were increased by increments of 0.25 m/yr, from  
 419 0.25 to 4.5 m/yr, resulting in 18 unique saturated zone transport rates to evaluate in the Random Forest model. The range of  
 420 transport rates suggested by groundwater age dating was large (more than an order of magnitude) and are considered to include  
 421 rates likely to be expected in a variety of field settings. Presumably, similar model constraints and results could have been obtained  
 422 without the prior age data and with some relatively conservative estimates.

423 Travel times  $\tau_u$  and  $\tau_s$  were calculated for each well based on  $z_u$  and  $z_s$ , respectively. For every possible combination of  
424 vadose and saturated zone transport rates, a unique total travel time,  $\tau_t$ , was calculated for each well based on the vadose and  
425 saturated zone dimensions of that particular well.

$$426 \tau_t = \tau_u + \tau_s, \tag{4}$$

427 The total travel times from Equation 4 were used to lag dynamic predictors relative to each nitrate sample date. For  
428 instance, a nitrate sample collected in 2010 at a well with a 20-year total travel time (e.g.,  $\tau_u = 10$  yrs and  $\tau_s = 10$  yrs) would be  
429 assigned the 1990 values for precipitation (450 mm), Interstate Canal discharge (0.4 km<sup>3</sup>/yr), center pivot irrigated area (2,484  
430 hectares), and area of planted corn (8,905 hectares).

431 A total of 288 unique transport rate combinations (corresponding to different combinations of the 16 vadose and 18  
432 saturated zone transport rates) were joined into a single dataset totalling over 300,000 observations to determine the optimal rate  
433 resulting in the maximum testing NSE from the model. Each transport rate combination incorporated up to 1,049 groundwater  
434 [NO<sub>3</sub>⁻] values. To decrease runtime, Random Forest models were parallel processed through a Holland Computing Center (HCC)  
435 cluster at the University of Nebraska-Lincoln.

### 436 3 Results and Discussion

437 This study addressed a relatively unexplored use of Random Forest, which was to identify optimal lag times based on  
438 testing a range of transport rate combinations through the vadose and saturated zones, historical [NO<sub>3</sub>⁻], and the use of easily  
439 accessible environmental datasets.

#### 440 3.1. Relative Importance of Transport Time and Dynamic Variables

441 In our initial modelling with (using both static and dynamic predictors), we anticipated that we could use the Random  
442 Forest model with the highest NSE to identify the optimal pair of vadose and saturated-zone transport rates. However, no clear  
443 pattern emerged among the different models (Fig. 4). Given the small differences and lack of defined pattern in testing NSE values,  
444 we selected ten transport rate combinations (the five top performing models, plus four transport rate combinations of high and low  
445 transport rates, and one intermediate transport rate combination) for further evaluation of variable importance and sensitivity to a  
446 range of transport rate combinations (Table 2). Median total travel time ranked third in variable importance, while the four dynamic  
447 variables consistently had the four lowest rankings (Fig. 5). Total travel time also had the greatest variability in importance among  
448 the fifteen variables, with a range of 18.4% between the upper and lower values, suggesting some model sensitivity to lag times.  
449 Excluding total travel time, the remaining variables had an average variable importance range of 6%.

450 Dynamic variables had little influence on the model, despite common potential linkages to groundwater [NO<sub>3</sub>⁻] (Böhlke  
451 et al., 2007; Exner et al., 2010; Spalding et al., 2001). A pattern emerged among dynamic variables where the stronger the historical  
452 trend of the predictor, the greater the importance of the predictor (Fig. 3; Fig. 5). For instance, center pivot irrigated area (highest  
453 ranking dynamic variable) had the least noise and the most pronounced trend, while annual precipitation (lowest ranking variable)  
454 was highly variable and lacked any trend over time (Fig. 3), and also may not be a substantial source of recharge (Böhlke et al.,  
455 2007). Further exploration could be done to test more refined variables and/or spatially varying predictors – for instance, annual  
456 median rainfall intensity for the growing season might have a more direct connection to nitrate leaching than total annual  
457 precipitation. However, rainfall intensity data are not readily available. Likewise, availability of a long-term, detailed fertilizer  
458 loading dataset would be advantageous in providing a more substantiated conclusion regarding the viability of applying dynamic  
459 variables to determine vadose and saturated-zone lag. Dynamic variables could be of more use in other study areas that undergo

Formatted: Indent: First line: 0.5"

460 relatively rapid and pronounced changes (e.g., land use). In future work, the model sensitivity to dynamic variables could be tested  
461 through formal sensitivity analysis and/or automated variable selection algorithms (Eibe et al., 2016).

462 Ultimately, results from initial analyses suggest that (1) the dynamic data did little to improve model performance, and  
463 (2) Random Forest was not able to relate the four considered dynamic predictors to  $[\text{NO}_3^-]$  in a meaningful way that could be used  
464 to estimate lag time. It is likely the influence of these dynamic predictors is dampened as nitrate is transported from the surface to  
465 wells such that data-driven approaches are unable to sort through noise to identify relationships.

### 466 3.2 Use of Random Forest to determine transport rates

467 Due to their low relative importance as predictors, all four dynamic predictors were removed in the subsequent analysis.  
468 As discussed above, a notable variation in total travel time  $\%_{\text{incMSE}}$  was observed in Fig. 5, suggesting model sensitivity to this  
469 variable. Additionally, a relationship between travel time and  $[\text{NO}_3^-]$  has been suggested in the Dutch Flats area through previous  
470 studies (Böhlke et al., 2007; Wells et al., 2018). Therefore, a second analysis of just the 11 static predictors was performed over  
471 the full range of vadose and saturated transport rates (i.e., 288 combinations). However, in the second analysis, model sensitivity  
472 to total travel time – evaluated with respect to the transport rate combination corresponding to the largest  $\%_{\text{incMSE}}$  of total travel  
473 time – was used to determine a distinguished transport rate combination. In other words, models were re-trained and tested for all  
474 transport rate combinations, each of which produced a unique set of values for the total travel time variable. As described in Section  
475 2.3.5, the  $\%_{\text{incMSE}}$  value for total travel time was then based on the error induced in the model by permuting the calculated total  
476 travel times across all the nitrate observations (i.e., randomly shuffling the total travel time variable, and thus disturbing the  
477 structure of the dataset).

478 The Random Forest models were useful in identifying the relative magnitudes of  $V_u$  and  $V_s$  that led to high  $\%_{\text{incMSE}}$ .  
479 Based on the heat map of  $\%_{\text{incMSE}}$ , a band of transport rate combinations with consistently high  $\%_{\text{incMSE}}$  was visually apparent  
480 (Fig. 6). The upper and lower bounds of the band translate to transport rate ratios ( $V_s/V_u$ ) ranging from 0.9 to 1.5, and are values  
481 that could be useful in constraining recharge and/or transport rate estimates in more complex mechanistic models [of the Dutch](#)  
482 [Flats area](#), as part of a hybrid modelling approach. This is especially important because recharge is one of the most sensitive  
483 parameters in a groundwater model (Mittelstet et al., 2011), yet one with high uncertainty. Whereas a saturated-zone velocity that  
484 is greater than a vadose-zone velocity would be unexpected in many unconsolidated surficial aquifers receiving distributed  
485 recharge, the statistical machine learning results are consistent with two contrasting primary recharge processes in the Dutch Flats  
486 area: (1) diffuse recharge from irrigation and precipitation across the landscape, and (2) focused recharge from leaking irrigation  
487 conveyance canals.

488 The  $\%_{\text{incMSE}}$  of total travel time in the second analysis [\(using only static variables\)](#) ranged from 20.6 to 31.5%, with the  
489 largest  $\%_{\text{incMSE}}$  associated with vadose and saturated-zone transport rates of 3.50 m/yr and 3.75 m/yr, respectively (Fig. 6), and  
490 the top four predictors for this transport rate combination were total travel time, vadose-zone thickness, dissolved oxygen, and  
491 saturated thickness (Fig. 7). Converting those vadose and saturated-zone transport rates to recharge rates yielded values of 0.46  
492 m/yr and 1.31 m/yr, respectively. Such a large difference between the two recharge values is consistent with the hydrologic  
493 conceptual model of the Dutch Flats area. In fact, both model recharge rates compare favourably with recharge rates calculated  
494 from the previous Dutch Flats studies using  $^3\text{H}/^3\text{He}$  age-dating (Böhlke et al., 2007; Wells et al., 2018). For instance, the recharge  
495 rate determined from the vadose-zone transport rate in this study (0.46 m/yr) was comparable to the mean recharge rate of 0.38  
496 m/yr ( $n = 9$ ) from groundwater age-dating at shallow wells, which are most representative of diffuse recharge below crop fields  
497 that are present across most of the study area (e.g., Figure S2). Additionally, the recharge rate (1.31 m/yr) determined from the  
498 saturated-zone transport rate was consistent with the mean recharge value derived from groundwater ages in intermediate wells

499 (1.22 m/yr, n = 13; Böhlke et al., 2007; Wells et al., 2018). Intermediate wells are variably impacted by focused recharge from  
500 canals in upgradient areas. Given the similarity in diffuse recharge and focused recharge estimates from both Random Forest and  
501 groundwater age-dating, the transport rate ratios (1.2 and 1.1, respectively) were consistent. That is, the Random Forest modelling  
502 framework produced transport rates consistent with the major hydrological processes in Dutch Flats both in direct (i.e., transport  
503 rate estimates) and relative (i.e., transport rate ratio) terms.

504 Assuming the Random Forest approach has accurately captured the two major recharge processes (diffuse recharge over  
505 crop fields and focused recharge from canals), a comparison of recharge rates from all sampled groundwater wells representative  
506 of recharge to the groundwater system as a whole (0.84 m/yr, n = 43) to the recharge rates from Random Forest modelling (0.46  
507 and 1.31 m/yr) would provide an estimate of the relative importance of diffuse versus focused recharge on overall recharge in  
508 Dutch Flats. Under these assumptions, diffuse recharge would account for approximately 55%, while focused recharge would  
509 account for about 45% of total recharge in the Dutch Flats area. Similarly, Böhlke et al. (2007) concluded that these two recharge  
510 sources contributed roughly equally to the aquifer on the basis of groundwater age profiles, as well as from dissolved atmospheric  
511 gas data indicating mean recharge temperatures between those expected of diffuse infiltration and focused canal leakage.

512 Partial dependence plots, which illustrate the impact a single predictor has on  $[\text{NO}_3^-]$  in the model with respect to other  
513 predictors (Fig. 8), largely reflect the conceptual understanding of the system from previous studies including Böhlke et al. (2007)  
514 and Wells et al. (2018). Key features that strengthen confidence in the Random Forest modelling include (1) depth to bottom  
515 screen, where groundwater  $[\text{NO}_3^-]$  is lower at greater depths, (2) the effects of minor and major canals, where groundwater  $[\text{NO}_3^-]$   
516 in the vicinity of canals is diluted by canal leakage, and the influence of major canals extends a longer distance when compared to  
517 that of minor canals, (3) land surface elevation, where elevations indicating proximity to major canals are associated with relatively  
518 lower groundwater  $[\text{NO}_3^-]$ , and (4) DO concentration, where higher DO concentration is linked to higher groundwater  $[\text{NO}_3^-]$ . We  
519 note that decreasing DO and  $[\text{NO}_3^-]$  with groundwater age can be explained by DO reduction and historical changes in  $[\text{NO}_3^-]$   
520 recharge, whereas groundwater chemistry and nitrate isotopic data recorded in both this study and previous Dutch Flats studies  
521 suggest denitrification was not a major factor in this alluvial aquifer.

522 The partial dependence plot (Fig. 8) for total travel time exhibits a pronounced threshold, where  $[\text{NO}_3^-]$  is markedly higher  
523 for groundwater with travel time less than seven years. It is possible this reflects long-term stratification of groundwater  $[\text{NO}_3^-]$ ,  
524 stemming from the suggested patterns stated above as nitrate varies with aquifer depth due to the influences of diffuse and focused  
525 recharge in the region. This seven-year threshold is slightly lower than a previous estimate of mean groundwater age in the aquifer  
526 (8.8 years; Böhlke et al., 2007; where groundwater age excludes vadose-zone travel time) and suggests that shallow groundwater  
527 can respond relatively rapidly to changes in nitrogen management in the Dutch Flats area.

### 528 3.3 Opportunities and limitations of Random Forest approach in estimating lag times

529 Overall, results suggest that in a complex system such as Dutch Flats, Random Forest was able to identify reasonable  
530 transport rates for both the vadose and saturated zones, and with additional validation, this method may offer an inexpensive (i.e.,  
531 compared to groundwater age-dating across a large monitoring well network and/or complex modelling) and reasonable technique  
532 for estimating lag time from historical monitoring data. Further, this approach allows for additional insight on groundwater  
533 dynamics to be extracted from existing monitoring data. However, this study was conducted in the context of a larger project  
534 (Wells et al., 2018) and built on prior research on groundwater flow and  $[\text{NO}_3^-]$  in the study area (Böhlke et al., 2007). Therefore,  
535 it is critical in future work to incorporate site-specific knowledge, process understanding, and approaches for increasing  
536 interpretability of machine learning models (Lundberg et al., 2020, Saia et al., 2020), as highlighted in key considerations below.  
537

538 Some key considerations for future application of this approach include:

- 539 (1) The Random Forest approach might be useful for estimating future recharge and  $[\text{NO}_3^-]$  using multiple potential  
540 management scenarios, as long as considered management scenarios fall within the range of historical observations used  
541 to train the model. This information could be used to inform policy makers of the impact that current and future  
542 management decisions will have on recharge and  $[\text{NO}_3^-]$ .
- 543 (2) The Dutch Flats overlies a predominantly oxic aquifer, where nitrate transport is mostly conservative. In aquifers with  
544 ~~both oxic and anoxic conditions~~ heterogeneity in denitrification potential and/or distinct nitrate extinction depths (Liao  
545 et al., 2012; Welch et al., 2011), this approach may be biased toward oxic portions of the aquifer where the nitrate signal  
546 is preserved. Similarly, vertical profiles of  $[\text{NO}_3^-]$  and isotopic composition in the vadose zone could provide valuable  
547 data to investigate (1) the amount of nitrate stored in the vadose zone, and (2) whether nitrate undergoes any  
548 biogeochemical changes while being transported through the vadose zone to the water table.
- 549 (3) While estimates of vadose and saturated-zone transport rates determined from  $\%_{\text{inc}}\text{MSE}$  are consistent with previous  
550 studies, the predictive performance of the selected model (based on NSE and visual inspection of predicted versus  
551 observed nitrate plots) was not substantially different than other models tested. In other words, the “optimal model” was  
552 only weakly preferred in terms of predicting  $[\text{NO}_3^-]$ . Testing the approach of using  $\%_{\text{inc}}\text{MSE}$  in other vadose and saturated  
553 zones, with substantial comparison to previous transport rate estimates, is warranted. This would be especially valuable  
554 in an area with a well-defined input function for nitrate that could be compared to a reconstructed input function from the  
555 model. Further, in aquifer settings with relatively evenly distributed recharge, optimized travel times to wells could be  
556 used to estimate the infiltration date of samples, thus providing an optimized view of historical variation of  $[\text{NO}_3^-]$  entering  
557 the subsurface, as illustrated in Figure S1B. In the Dutch Flats area, however, such an analysis is complicated by effects  
558 of subsurface nitrate dilution by local recharge from canal leakage.
- 559 (4) Despite potential non-uniqueness in prediction metrics, the heat map of  $\%_{\text{inc}}\text{MSE}$  did reveal an orderly pattern suggesting  
560 consistent transport rate ratios. For modelling efforts where recharge rates are a key calibration parameter, identification  
561 of a range of reasonable recharge rates, and/or the ratio of recharge rates from diffuse and focused recharge sources for a  
562 complex system will reduce model uncertainty and improve results. This statistical machine learning approach, which  
563 essentially leverages nitrate as a tracer (albeit with an unknown input function in this case), may provide valuable insight  
564 to complement relatively expensive groundwater age-dating or vadose-zone monitoring data, or perhaps as a standalone  
565 approach for first-order approximations.
- 566 (5) The demonstrated statistical machine learning approach is apparently well-suited for drawing out transport rate  
567 information from a site with two distinct recharge sources (diffuse versus focused recharge sources) driving the  
568 groundwater nitrate dynamics. Further testing is needed at sites where recharge and nitrate dynamics are more subtle.

#### 569 **4 Conclusions**

570 The Dutch Flats area exhibits large variations in  $[\text{NO}_3^-]$  throughout a relatively small region in western Nebraska. Long-  
571 term groundwater  $[\text{NO}_3^-]$  monitoring and previous groundwater age-dating studies in Dutch Flats provided an opportune setting to  
572 test a new application of statistical machine learning (Random Forest) for determining vadose and saturated-zone transport rates.  
573 Overall results suggest Random Forest has the capability to both identify reasonable transport rates (and lag time) and key variables  
574 influencing groundwater  $[\text{NO}_3^-]$ , albeit with potential for non-unique results. Limitations were also identified when using dynamic  
575 predictors to model groundwater  $[\text{NO}_3^-]$ . Utilizing only static predictors, and Random Forest’s ability to evaluate variable

576 importance, vadose-zone and saturated-zone transport rates were selected based on model sensitivity to changing the total travel  
577 time predictor. In other words, total travel time variable importance was evaluated for 288 different transport rate combinations,  
578 and the combination with a total travel time having the largest influence over the model's ability to predict [NO<sub>3</sub><sup>-</sup>] was selected for  
579 additional examination. This analysis identified a vadose-zone and saturated-zone transport rate combination consistent with rates  
580 previously estimated from <sup>3</sup>H/<sup>3</sup>He age-dating in Böhlke et al. (2007) and Wells et al. (2018), indicating a combination of distributed  
581 and focused sources of irrigation recharge to this aquifer

582 Future studies ~~should could~~ include assessments of the proper conditions for application of dynamic predictors and include  
583 comparisons of data-driven analyses with complementary datasets [and/or modelling \(e.g., field-based recharge rate estimates,](#)  
584 [finite-difference flow model\)](#). Despite noted limitations, partial dependence plots and relative importance of predictors were largely  
585 consistent with previous findings and mechanistic understanding of the study area, giving greater confidence in model outputs.  
586 The influence of canal leakage on groundwater recharge rates and [NO<sub>3</sub><sup>-</sup>], for example, was consistent with previous Dutch Flats  
587 studies. Partial dependence plots suggest a threshold of higher [NO<sub>3</sub><sup>-</sup>] for groundwater with total travel time (vadose and saturated-  
588 zone travel times, combined) of less than seven years, indicating the potential for relatively rapid groundwater [NO<sub>3</sub><sup>-</sup>] response to  
589 widespread implementation of best management practices. Additionally, research is needed to determine the minimum number of  
590 observations needed to effectively apply the framework shown here.

591  
592 **Author contribution:** TG, AM, and NN were responsible for conceptualization. MW and NN developed the model code and MW  
593 performed formal analysis. MW prepared the manuscript from his M.S. thesis with contributions from all co-authors, including  
594 JKB. TG was responsible for project administration and funding acquisition.

595  
596 **Acknowledgements:** The authors acknowledge the North Platte Natural Resources District for providing technical assistance and  
597 resources, including long-term groundwater nitrate data accessed via the Quality-Assessed Agrichemical Contaminant Database  
598 for Nebraska Groundwater. We thank Steve Sibray and Mason Johnson for their support in field sampling efforts and Les Howard  
599 for cartography. ~~Models were run on the Holland Computing Center (HCC) cluster at the University of Nebraska-Lincoln.~~ We  
600 also thank Christopher Green, Sophie Ehrhardt, ~~and an Pia Ebeling, and two~~ anonymous reviewers for helpful comments on earlier  
601 versions of the paper. Any use of trade, firm, or product names is for descriptive purposes only and does not imply endorsement  
602 by the U.S. Government.

603  
604  
605 **Funding:** This work was supported by the U.S. Geological Survey 104b Program (Project 2016NE286B), U.S. Department of  
606 Agriculture—National Institute of Food and Agriculture NEB-21-177 (Hatch Project 1015698), and Daugherty Water for Food  
607 Global Institute Graduate Student Fellowship.

608 **Supplemental Material:** [An online file accompanying this article contains additional figures, tables, and details of methods used](#)  
609 [for the study.](#)

611  
612 **Code and Data Availability:** Code is available on request. Data used in the random forest model and described in the supplemental  
613 [information—material](#) is available via the University of Nebraska – Lincoln Data Repository  
614 (<https://doi.org/10.32873/unl.dr.20200428>).

Formatted: Font color: Text 1  
Formatted: Font: Bold, Font color: Text 1, Not Highlight  
Formatted: Font color: Text 1, Not Highlight  
Formatted: Font color: Text 1

615 **References**

- 616 Anning, D. W., Paul, A. P., McKinney, T. S., Huntington, J. M., Bexfield, L. M. and Thiros, S. A.: Predicted Nitrate ~~And and~~  
617 Arsenic Concentrations ~~In in~~ Basin-Fill Aquifers ~~Of of F~~ the Southwestern United States. ~~Report~~, United States Geological Survey  
618 ~~Scientific Investigations Report 2012-5065, 78 p.~~, [online] Available from: <https://pubs.usgs.gov/sir/2012/5065/>, 2012.
- 619 Babcock, H. M., Visher, F. N. and Durum, W. H.: Ground-Water Conditions ~~In in The the~~ Dutch Flats ~~areaArea~~, Scotts Bluff ~~And~~  
620 ~~and~~ Sioux Counties, Nebraska, ~~with a section on chemical quality of the ground water~~, ~~United States Geological Survey Circular~~  
621 ~~126, 51 p.~~, ~~Report~~. [online] Available from: <http://pubs.er.usgs.gov/publication/cir126>, 1951.
- 622 Ball, L. B., Kress, W. H., Steele, G. V., Cannia, J. C. and Andersen, M. J.: Determination ~~Of of~~ Canal Leakage Potential Using  
623 Continuous Resistivity Profiling Techniques, Interstate ~~And and~~ Tri-State Canals, Western Nebraska ~~And and~~ Eastern Wyoming,  
624 2004, ~~United States Geological Survey- Scientific Investigations Report 2006-5032, 53 p.~~, ~~Report, United States Geological~~  
625 ~~Survey~~. [online] Available from: <http://pubs.er.usgs.gov/publication/sir20065032>, 2006.
- 626 Böhlke, J. K.: Groundwater Recharge ~~And and~~ Agricultural Contamination, *Hydrogeology Journal*, 10(1), 153–179,  
627 doi:10.1007/s10040-001-0183-3, 2002.
- 628 Böhlke, J. K. and Denver, J. M.: Combined Use of Groundwater Dating, Chemical, and Isotopic Analyses to Resolve the History  
629 and Fate of Nitrate Contamination in Two Agricultural Watersheds, Atlantic Coastal Plain, Maryland, *Water Resources Research*,  
630 31(9), 2319–2339, doi:10.1029/95WR01584, 1995.
- 631 Böhlke, J. K., Wanty, R., Tuttle, M., Delin, G. and Landon, M.: Denitrification ~~In in The the~~ Recharge Area ~~And and~~ Discharge  
632 Area ~~Of of A a~~ Transient Agricultural Nitrate Plume ~~In in A a~~ Glacial Outwash Sand Aquifer, Minnesota: ~~Denitrification in~~  
633 ~~recharge and discharge areas~~, *Water Resources Research*, 38(7), 10-1-10-26, doi:10.1029/2001WR000663, 2002.
- 634 Böhlke, J. K., Verstraeten, I. M. and Kraemer, T. F.: Effects ~~Of of~~ Surface-Water Irrigation ~~On on~~ Sources, Fluxes, ~~And and~~  
635 Residence Times ~~Of of~~ Water, Nitrate, ~~And and~~ Uranium ~~In in An an~~ Alluvial Aquifer, *Applied Geochemistry*, 22(1), 152–174,  
636 doi:10.1016/j.apgeochem.2006.08.019, 2007.
- 637 Breiman, L.: Random Forests, *Machine Learning*, 45(1), 5–32, doi:10.1023/A:1010933404324, 2001.
- 638 Browne, B. A. and Guldan, N. M.: Understanding Long-Term Baseflow Water Quality Trends Using a Synoptic Survey of the  
639 Ground Water–Surface Water Interface, Central Wisconsin, *Journal of Environment Quality*, 34(3), 825,  
640 doi:10.2134/jeq2004.0134, 2005.
- 641 Cherry, M., Gilmore, T., Mittelstet, A., Gastmans, D., Santos, V. and Gates, J. B.: Recharge Seasonality Based ~~On on~~ Stable  
642 Isotopes: Nongrowing Season Bias Altered ~~By by~~ Irrigation ~~In in~~ Nebraska, *Hydrological Processes*, doi:10.1002/hyp.13683, 2020.
- 643 Cook, P. G. and Böhlke, J. K.: Determining Timescales for Groundwater Flow and Solute Transport, in *Environmental Tracers in*  
644 *Subsurface Hydrology*, edited by P. G. Cook and A. L. Herczeg, pp-1–30, Springer US, Boston, MA., 2000.
- 645 Dieter, C. A., Maupin, M. A., Caldwell, R. R., Harris, M. A., Ivahnenko, T. I., Lovelace, J. K., Barber, N. L. and Linsey, K. S.:  
646 Estimated Use ~~Of of~~ Water ~~In in~~ The United States ~~In in~~ 2015, ~~United States Geological Survey Circular 1441, 65 p.~~, [online]  
647 ~~Available from: https://doi.org/10.3133/cir1441Report, Reston, VA.~~, 2018.
- 648 Eberts, S. M., Thomas, M. S. and Jagucki, M. L.: ~~The quality of our Nation's waters—Factors affecting~~ ~~Affecting public~~  
649 ~~supply~~ ~~Supply-well Well~~ ~~vulnerability~~ ~~Vulnerability to contamination~~ ~~Contamination:—Understanding observed~~ ~~Observed water~~  
650 ~~Water quality~~ ~~Quality~~ and ~~anticipating~~ ~~Anticipating future~~ ~~Future water~~ ~~Water quality~~ ~~Quality~~, U.S. Geological Survey Circular  
651 1385, ~~120 p.~~, [online] Available from: <https://pubs.usgs.gov/circ/1385/>, 2013.
- 652 Efron, B.: Bootstrap Methods: Another Look at the Jackknife, *The Annals of Statistics*, 7(1), 1–26, doi:10.1214/aos/1176344552,  
653 1979.
- 654 Eibe, F., Hall, M. A. and Witten, I. H.: The WEKA Workbench, in Online Appendix for “Data Mining: Practical Machine Learning  
655 Tools and Techniques,” Morgan Kaufmann., 2016.
- 656 Exner, M. E., Perea-Estrada, H. and Spalding, R. F.: Long-Term Response of Groundwater Nitrate Concentrations to Management  
657 Regulations in Nebraska’s Central Platte Valley, *The Scientific World Journal*, 10, 286–297, doi:10.1100/tsw.2010.25, 2010.



658 Gilmore, T. E., Genereux, D. P., Solomon, D. K. and Solder, J. E.: Groundwater Transit Time Distribution ~~And-and~~ Mean ~~From~~  
659 ~~from~~ Streambed Sampling ~~In-in An-an~~ Agricultural Coastal Plain Watershed, North Carolina, ~~UsaUSA:-Groundwater-transit-time,~~  
660 Water Resources Research, 52(3), 2025–2044, doi:10.1002/2015WR017600, 2016.

661 Green, C. T., Liao, L., Nolan, B. T., Juckem, P. F., Shope, C. L., Tesoriero, A. J. and Jurgens, B. C.: Regional Variability of Nitrate  
662 Fluxes in the Unsaturated Zone and Groundwater, Wisconsin, USA, Water Resources Research, 54(1), 301–322,  
663 doi:10.1002/2017WR022012, 2018.

664 Harvey, F. E. and Sibray, S. S.: Delineating Ground Water Recharge from Leaking Irrigation Canals Using Water Chemistry and  
665 Isotopes, Ground Water, 39(3), 408–421, doi:10.1111/j.1745-6584.2001.tb02325.x, 2001.

666 Hastie, T., Tibshirani, R. and Friedman, J. H.: The Elements ~~Of-of~~ Statistical Learning: Data Mining, Inference, And Prediction,  
667 2nd ed., Springer, New York, NY., 2009.

668 Hobza, C. M. and Andersen, M. J.: Quantifying Canal Leakage Rates Using ~~A-a~~ Mass-Balance Approach ~~And-and~~ Heat-Based  
669 Hydraulic Conductivity Estimates ~~In-in~~ Selected Irrigation Canals, Western Nebraska, 2007 through 2009, ~~Report-~~United States  
670 Geological Survey ~~Scientific Investigations Report 2010-5226, 38 p., https://doi.org/10.3133/sir20105226.~~ [online] Available  
671 from: <http://pubs.er.usgs.gov/publication/sir20105226>, 2010.

672 Homer, C. G., Dewitz, J., Yang, L., Jin, S., Danielson, P., Xian, G. Z., Coulston, J., Herold, N., Wickham, J. and Megown, K.:  
673 Completion of the 2011 National Land Cover Database for ~~The~~ Conterminous United States – Representing ~~A-a~~ Decade ~~Of-of~~  
674 Land Cover Change Information, Photogrammetric Engineering and Remote Sensing, 81, 345354, 2015.

675 Hudson, C. (NPNRD): Personal Communication with M.J. Wells, University of Nebraska, Lincoln, NE, USA, 2018.

676 Ilampooranan, I., Van Meter, K. J. and Basu, N. B.: A Race ~~against-Against~~ Time: Modelling Time Lags in Watershed Response,  
677 Water Resources Research, doi:10.1029/2018WR023815, 2019.

678 Irmak, S., Odhiambo, L., Kranz, W. L. and Eisenhauer, D. E.: Irrigation Efficiency ~~And-and~~ Uniformity, And Crop Water Use  
679 Efficiency, Extension Circular, University of Nebraska – Lincoln, Lincoln, NE. [online] Available from: ~~Available-at~~  
680 <http://extensionpubs.unl.edu/>, 2011.

681 Jones, Z. M. and Linder, F. J.: Exploratory Data Analysis using Random Forests, in 73rd Annual MPSA Conference, ~~pp-~~1–31.  
682 [online] Available from: [http://zmjones.com/static/papers/rfss\\_manuscript.pdf](http://zmjones.com/static/papers/rfss_manuscript.pdf) (Accessed 25 May 2018), 2015.

683 Juntakut, P., Snow, D. D., Haacker, E. M. K. and Ray, C.: The Long Term Effect ~~Of-of~~ Agricultural, Vadose Zone ~~And-and~~  
684 Climatic Factors ~~On-on~~ Nitrate Contamination ~~In-in~~ Nebraska’s Groundwater System, Journal of Contaminant Hydrology, 220,  
685 33–48, doi:10.1016/j.jconhyd.2018.11.007, 2019.

686  
687 Kennedy, C. D., Genereux, D. P., Corbett, D. R. and Mitasova, H.: Spatial ~~And-and~~ Temporal Dynamics ~~Of-of~~ Coupled Groundwater  
688 ~~And-and~~ Nitrogen Fluxes Through ~~A-a~~ Streambed ~~In-in An-an~~ Agricultural Watershed: ~~Groundwater-and-nitrogen-fluxes-in-a~~  
689 ~~streambed~~, Water Resources Research, 45(9), doi:10.1029/2008WR007397, 2009.

690 Knoll, L., Breuer, L. and Bach, M.: Nation-Wide Estimation ~~Of-of~~ Groundwater Redox Conditions ~~And-and~~ Nitrate Concentrations  
691 Through Machine Learning, Environmental Research Letters, 15(6), 064004, doi:10.1088/1748-9326/ab7d5c, 2020.

692  
693 Kuhn, M.: Building Predictive Models in R Using the ~~caret-Caret~~ Package, Journal of Statistical Software, 28(5),  
694 doi:10.18637/jss.v028.i05, 2008.

695 Liao, L., Green, C. T., Bekins, B. A. and Böhlke, J. K.: Factors Controlling Nitrate Fluxes ~~In-in~~ Groundwater ~~In-in~~ Agricultural  
696 Areas: ~~Factors-controlling-nitrate-fluxes-in-groundwater~~, Water Resources Research, 48(6), doi:10.1029/2011WR011008, 2012.

697 Luckey, R. R. and Cannia, J. C.: Groundwater Flow Model of the Western Model Unit of the Nebraska Cooperative Hydrology  
698 Study (COHYST) Area, Nebraska Department of Natural Resources, Lincoln, NE. [online] Available from:  
699 [ftp://ftp.dnr.nebraska.gov/Pub/cohystftp/cohyst/model\\_reports/WMU\\_Documentation\\_060519.pdf](ftp://ftp.dnr.nebraska.gov/Pub/cohystftp/cohyst/model_reports/WMU_Documentation_060519.pdf), 2006.

700 Lundberg, S. M., Erion, G., Chen, H., DeGrave, A., Prutkin, J. M., Nair, B., Katz, R., Himmelfarb, J., Bansal, N. and Lee, S. -I.:  
701 from Local Explanations ~~To-to~~ Global Understanding with Explainable ~~AI-AI For-for~~ Trees, Nature Machine Intelligence, 2(1), 56–  
702 67, doi:10.1038/s42256-019-0138-9, 2020.

703  
704 McMahon, P. B., Dennehy, K. F., Bruce, B. W., Böhlke, J. K., Michel, R. L., Gurdak, J. J. and Hurlbut, D. B.: Storage ~~And~~  
705 Transit Time ~~Of~~ Chemicals ~~In~~ Thick Unsaturated Zones Under Rangeland ~~And~~ Irrigated Cropland, High Plains, United  
706 States: ~~Chemical storage in thick unsaturated zone~~, Water Resources Research, 42(3), doi:10.1029/2005WR004417, 2006.

707 Meals, D. W., Dressing, S. A. and Davenport, T. E.: Lag Time in Water Quality Response to Best Management Practices: A  
708 Review, Journal of Environment Quality, 39(1), 85, doi:10.2134/jeq2009.0108, 2010.

709 Mittelstet, A. R., Smolen, M. D., Fox, G. A. and Adams, D. C.: Comparison of Aquifer Sustainability Under Groundwater  
710 Administrations in Oklahoma and Texas: ~~Comparison of Aquifer Sustainability Under Groundwater Administrations in Oklahoma~~  
711 ~~and Texas~~, JAWRA—Journal of the American Water Resources Association, 47(2), 424–431, doi:10.1111/j.1752-  
712 1688.2011.00524.x, 2011.

713 Morgenstern, U., Daughney, C. J., Leonard, G., Gordon, D., Donath, F. M. and Reeves, R.: Using Groundwater Age ~~And~~  
714 Hydrochemistry ~~To~~ Understand Sources ~~And~~ Dynamics ~~Of~~ Nutrient Contamination Through ~~The~~ Catchment Into Lake  
715 Rotorua, New Zealand, Hydrology and Earth System Sciences, 19(2), 803–822, doi:10.5194/hess-19-803-2015, 2015.

716 Nash, J. E. and Sutcliffe, J. V.: River Flow Forecasting Through Conceptual Models Part I — A Discussion ~~Of~~ Principles,  
717 Journal of Hydrology, 10(3), 282–290, doi:10.1016/0022-1694(70)90255-6, 1970.

718 NASS: USDA/NASS QuickStats Ad-hoc Query Tool, [online] Available from: <https://quickstats.nass.usda.gov/> (Accessed 15  
719 February 2018), 2018.

720 NEDNR: Fifty-~~fifth~~ ~~Fifth~~ ~~biennial~~ ~~Biennial~~ ~~report~~ ~~Report~~ of the Department of Natural Resources, Nebraska Department of Natural  
721 Resources, Lincoln, NE. [online] Available from: [https://dnr.nebraska.gov/sites/dnr.nebraska.gov/files/doc/surface-](https://dnr.nebraska.gov/sites/dnr.nebraska.gov/files/doc/surface-water/biennial-reports/BiennialReport2005-06.pdf)  
722 [water/biennial-reports/BiennialReport2005-06.pdf](https://dnr.nebraska.gov/sites/dnr.nebraska.gov/files/doc/surface-water/biennial-reports/BiennialReport2005-06.pdf), 2009.

723 Nelson, N. G., Muñoz-Carpena, R., Philips, E. J., Kaplan, D., Sucsy, P. and Hendrickson, J.: Revealing Biotic and Abiotic Controls  
724 of Harmful Algal Blooms in a Shallow Subtropical Lake through Statistical Machine Learning, Environmental Science &  
725 Technology, 52(6), 3527–3535, doi:10.1021/acs.est.7b05884, 2018.

726 NOAA: National Climatic Data Center (NCDC), [online] Available from: <https://www.ncdc.noaa.gov/cdo-web/datatools>  
727 (Accessed 4 August 2017), 2017.

728 Nolan, B. T., Green, C. T., Juckem, P. F., Liao, L. and Reddy, J. E.: Metamodeling ~~And~~ Mapping ~~Of~~ Nitrate Flux ~~In~~ ~~The~~  
729 ~~the~~ Unsaturated Zone ~~And~~ ~~and~~ Groundwater, Wisconsin, ~~Usa~~ ~~USA~~, Journal of Hydrology, 559, 428–441,  
730 doi:10.1016/j.jhydrol.2018.02.029, 2018.

731 Nolan, B. T., Gronberg, J. M., Faunt, C. C., Eberts, S. M. and Belitz, K.: Modeling Nitrate at Domestic and Public-Supply Well  
732 Depths in the Central Valley, California, Environmental Science & Technology, 48(10), 5643–5651, doi:10.1021/es405452q,  
733 2014.

734 NRCS: Web Soil Survey. [online] Available from: <https://websoilsurvey.sc.egov.usda.gov/> (Accessed 16 November 2017), 2018.

735 Quedraogo, I., Defourny, P. and Vanclooster, M.: Validating ~~A~~ Continental-Scale Groundwater Diffuse Pollution Model Using  
736 Regional Datasets, Environmental Science and Pollution Research, doi:10.1007/s11356-017-0899-9, 2017.

737 Preston, T. (NPNRD): Personal Communication with M.J. Wells, University of Nebraska, Lincoln, NE, USA, 2017.

738 Puckett, L. J., Tesoriero, A. J. and Dubrovsky, N. M.: Nitrogen Contamination of Surficial Aquifers—A Growing Legacy-~~s~~,  
739 Environmental Science & Technology, 45(3), 839–844, doi:10.1021/es1038358, 2011.

740 R Core Team: R: A ~~language~~ ~~Language~~ and ~~environment~~ ~~Environment~~ for ~~statistical~~ ~~Statistical~~ ~~computing~~ ~~Computing~~, R  
741 Foundation for Statistical Computing, Vienna, Austria. [online] Available from: <https://www.R-project.org/>, 2017.

742 Rahmati, O., Choubin, B., Fathabadi, A., Coulon, F., Soltani, E., Shahabi, H., Mollaefar, E., Tiefenbacher, J., Cipullo, S., Ahmad,  
743 B. B. and Tien Bui, D.: Predicting Uncertainty ~~Of~~ Machine Learning Models ~~For~~ ~~for~~ Modelling Nitrate Pollution ~~Of~~  
744 Groundwater Using Quantile Regression ~~And~~ ~~Unee~~ ~~UNE~~ ~~EC~~ Methods, Science of The Total Environment, 688, 855–866,  
745 doi:10.1016/j.scitotenv.2019.06.320, 2019.

746  
747 Ransom, K. M., Nolan, B. T., A. Traum, J., Faunt, C. C., Bell, A. M., Gronberg, J. A. M., Wheeler, D. C., Z. Rosecrans, C.,  
748 Jurgens, B., Schwarz, G. E., Belitz, K., M. Eberts, S., Kourakos, G. and Harter, T.: A Hybrid Machine Learning Model ~~To~~  
749 Predict ~~And~~ Visualize Nitrate Concentration Throughout ~~The~~ Central Valley Aquifer, California, ~~Usa~~USA, Science of The  
750 Total Environment, 601–602, 1160–1172, doi:10.1016/j.scitotenv.2017.05.192, 2017.

751 Rodriguez-Galiano, V. F., Mendes, M. P., Garcia-Soldado, M. J., Chica-Olmo, M. and Ribeiro, L.: Predictive Modeling ~~Of~~  
752 Groundwater Nitrate Pollution Using Random Forest ~~And~~ Multisource Variables Related ~~To~~ Intrinsic ~~And~~ Specific  
753 Vulnerability: A Case Study ~~In~~ ~~An~~ Agricultural Setting (Southern Spain), Science of The Total Environment, 476–477, 189–  
754 206, doi:10.1016/j.scitotenv.2014.01.001, 2014.

755 Rossman, N. R., Zlotnik, V. A., Rowe, C. M. and Szilagyi, J.: Vadose Zone Lag Time ~~And~~ Potential 21st Century Climate  
756 Change Effects ~~On~~ Spatially Distributed Groundwater Recharge ~~In~~ The Semi-Arid Nebraska Sand Hills, Journal of  
757 Hydrology, 519, 656–669, doi:10.1016/j.jhydrol.2014.07.057, 2014.

758 Russoniello, C. J., Konikow, L. F., Kroeger, K. D., Fernandez, C., Andres, A. S. and Michael, H. A.: Hydrogeologic ~~controls~~  
759 ~~Controls~~ on ~~groundwater~~ Groundwater discharge ~~Discharge~~ and ~~nitrogen~~ Nitrogen loads ~~Loads~~ in a ~~eoastal~~ Coastal  
760 ~~watershed~~Watershed, Journal of Hydrology, 538, 783–793, doi:10.1016/j.jhydrol.2016.05.013, 2016.

761 Saia, S. M., Nelson, N., Huseth, A. S., Grieger, K. and Reich, B. J.: Transitioning Machine Learning from Theory to Practice in  
762 Natural Resources Management, Ecological Modelling, 435, 109257, doi:10.1016/j.ecolmodel.2020.109257, 2020.  
763

764 Spalding, R. F., Watts, D. G., Schepers, J. S., Burbach, M. E., Exner, M. E., Poreda, R. J. and Martin, G. E.: Controlling Nitrate  
765 Leaching in Irrigated Agriculture, Journal of Environment Quality, 30(4), 1184, doi:10.2134/jeq2001.3041184x, 2001.

766 Turkeltaub, T., Kurtzman, D. and Dahan, O.: Real-Time Monitoring ~~Of~~ Nitrate Transport ~~In~~ ~~The~~ Deep Vadose Zone Under  
767 ~~A~~ Crop Field – Implications ~~For~~ Groundwater Protection, Hydrology and Earth System Sciences, 20(8), 3099–3108,  
768 doi:10.5194/hess-20-3099-2016, 2016.

769 University of Nebraska-Lincoln (UNL): Quality-Assessed Agrichemical Contaminant Database for Nebraska Ground Water,  
770 [online] Available from: <https://clearinghouse.nebraska.gov/Clearinghouse.aspx> (Accessed 5 September 2016), 2016.

771 USBR: Hydromet: Archive Data Access, [online] Available from: [https://www.usbr.gov/gp/hydromet/hydromet\\_arcread.html](https://www.usbr.gov/gp/hydromet/hydromet_arcread.html)  
772 (Accessed 22 May 2018), 2018.

773 USDA: NAIP and NAPP Imagery, [online] Available from <https://dnr.nebraska.gov/data/digital-imagery> (Accessed 14 August  
774 2017), 2017

775 U.S. Geological Survey [USGS]: National Elevation Dataset (NED), [online] Available from: <https://datagateway.nrcs.usda.gov/>  
776 (Accessed 08 October 2020), 1997.

777 U.S. Geological Survey [USGS]: LANDSAT Imagery, [online] Available from: <https://earthexplorer.usgs.gov/> (Accessed 14  
778 August 2017), 2017.

779 U.S. Geological Survey [USGS]: NHDPlus High Resolution, [online] Available from: [https://nhd.usgs.gov/NHDPlus\\_HR.html](https://nhd.usgs.gov/NHDPlus_HR.html)  
780 (Accessed 29 June 2018), 2012.

781 Van Meter, K. J. and Basu, N. B.: Catchment Legacies and Time Lags: A Parsimonious Watershed Model to Predict the Effects  
782 of Legacy Storage on Nitrogen Export, edited by Y. Hong, PLoS ONE, 10(5), e0125971, doi:10.1371/journal.pone.0125971, 2015.

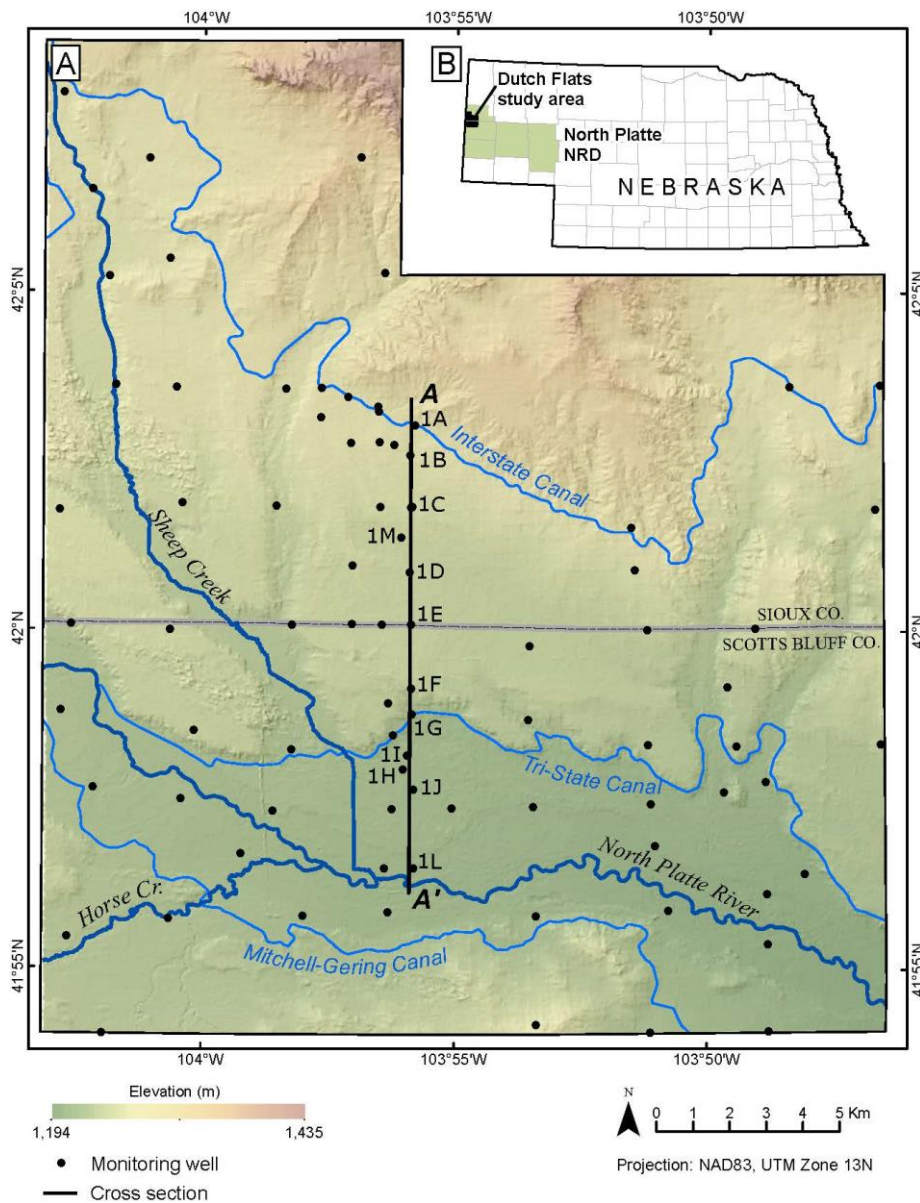
783 Van Meter, K. J. and Basu, N. B.: Time Lags ~~In~~ Watershed-Scale Nutrient Transport: An Exploration ~~Of~~ Dominant Controls,  
784 Environmental Research Letters, 12(8), 084017, doi:10.1088/1748-9326/aa7bf4, 2017.

785 Vanclooster, M., Petit, S., Bogaert, P. and Lietar, A.: Modelling Nitrate Pollution Vulnerability in the Brussel’s Capital Region  
786 (Belgium) Using Data-Driven Modelling Approaches, Journal of Water Resource and Protection, 12(05), 416–430,  
787 doi:10.4236/jwarp.2020.125025, 2020.  
788

789 Verstraeten, I. M., Sibray, S. S., Cannia, J. C. and Tanner, D. Q.: Reconnaissance of ~~ground~~Ground-water ~~Water~~ quality ~~Quality~~  
790 in the North Platte Natural Resources District, ~~western~~Western Nebraska, June-July 1991, ~~Report~~, United States Geological Survey

- 791 [Water-Resources Investigations Report 94-4057](https://doi.org/10.3133/wri944057), <https://doi.org/10.3133/wri944057>. [online] Available from:  
792 <http://pubs.er.usgs.gov/publication/wri944057>, 1995.
- 793 Verstraeten, I. M., Steele, G. V., Cannia, J. C., Böhlke, J. K., Kraemer, T. E., Hitch, D. E., Wilson, K. E. and Carnes, A. E.: Selected  
794 Field ~~And~~ Analytical Methods ~~And~~ Analytical Results ~~In in The the~~ Dutch Flats Area, Western Nebraska, 1995-99, ~~Report~~,  
795 United States Geological Survey [U.S. Geological Survey Open-File Report 00-413](https://doi.org/10.3133/ofr00413), 53 p, <https://doi.org/10.3133/ofr00413>, ~~Reston,~~  
796 ~~VA~~. [online] Available from: <http://pubs.er.usgs.gov/publication/ofr00413>, 2001a.
- 797 Verstraeten, I. M., Steele, G. V., Cannia, J. C., Hitch, D. E., Scriptor, K. G., Böhlke, J. K., Kraemer, T. F. and Stanton, J. S.:  
798 Interaction ~~Of of~~ Surface Water ~~And and~~ Ground Water ~~In in The the~~ Dutch Flats Area, Western Nebraska, 1995-99, ~~Report~~, United  
799 States Geological Survey [Water-Resources Investigations Report 01-4070](https://doi.org/10.3133/wri014070), 56 p, <https://doi.org/10.3133/wri014070>. [online]  
800 Available from: <http://pubs.er.usgs.gov/publication/wri014070>, 2001b.
- 801 Welch, H. L., Green, C. T. and Coupe, R. H.: The Fate ~~And and~~ Transport ~~Of of~~ Nitrate ~~In in~~ Shallow Groundwater ~~In in~~  
802 Northwestern Mississippi, USA, *Hydrogeology Journal*, 19(6), 1239–1252, doi:10.1007/s10040-011-0748-8, 2011.
- 803 Wells, M., Gilmore, T., Mittelstet, A., Snow, D. and Sibray, S.: Assessing Decadal Trends of a Nitrate-Contaminated Shallow  
804 Aquifer in Western Nebraska Using Groundwater Isotopes, Age-Dating, and Monitoring, *Water*, 10(8), 1047,  
805 doi:10.3390/w10081047, 2018.
- 806 Wheeler, D. C., Nolan, B. T., Flory, A. R., DellaValle, C. T. and Ward, M. H.: Modeling Groundwater Nitrate Concentrations ~~In~~  
807 ~~in~~ Private Wells ~~In in~~ Iowa, *Science of The Total Environment*, 536, 481–488, doi:10.1016/j.scitotenv.2015.07.080, 2015.
- 808 Yonts, D.: G02-1465 Crop Water Use in Western Nebraska, University of Nebraska-Lincoln Extension, [online] Available from:  
809 <https://digitalcommons.unl.edu/extensionhist>, 2002.
- 810 Young, L.A. (UNL): Personal Communication with M.J. Wells, University of Nebraska, Lincoln, NE, USA, 2016.

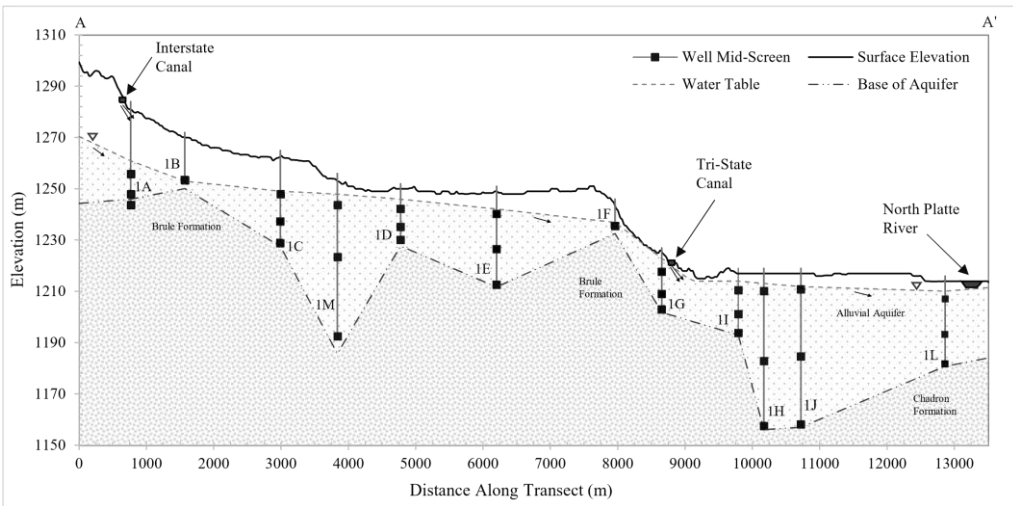
811



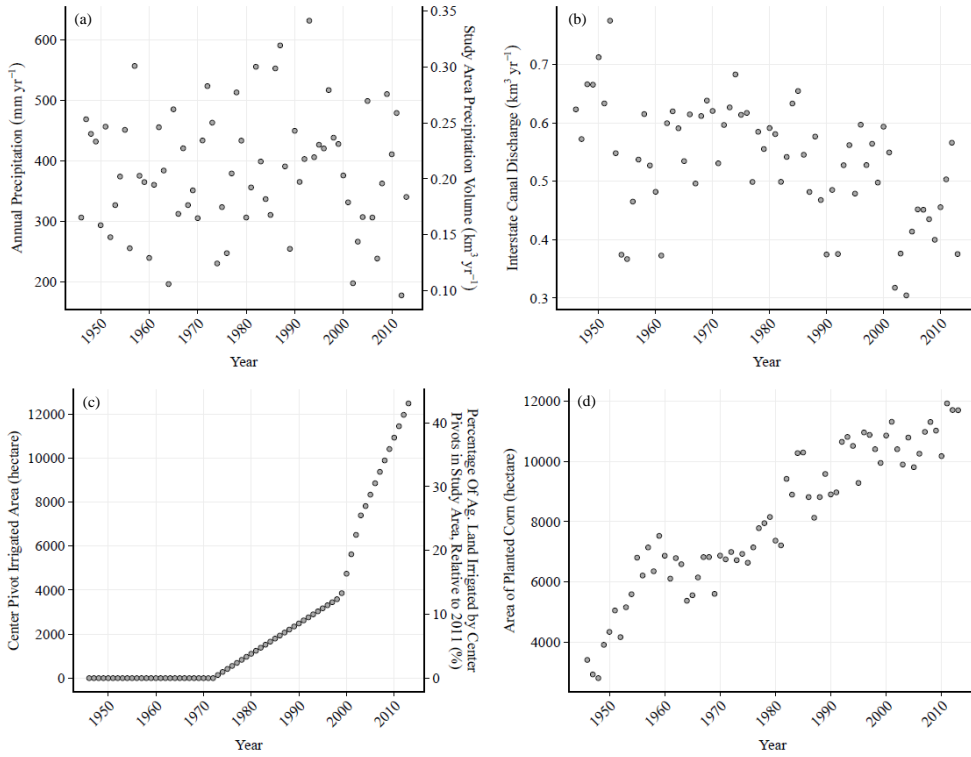
812  
 813 **Figure 1: Dutch Flats study area (A) overlain by 30 m Digital Elevation Model (USGS, 1997). The study area is located within the North**  
 814 **Platte Natural Resources District of western Nebraska (B). Depending on data availability, multiple wells (well nest) or a single well may**  
 815 **be found at each monitoring well location. Transect A-A' represents the location and wells displayed in the Fig. 2 hydrogeologic cross-**  
 816 **section.**

817

818

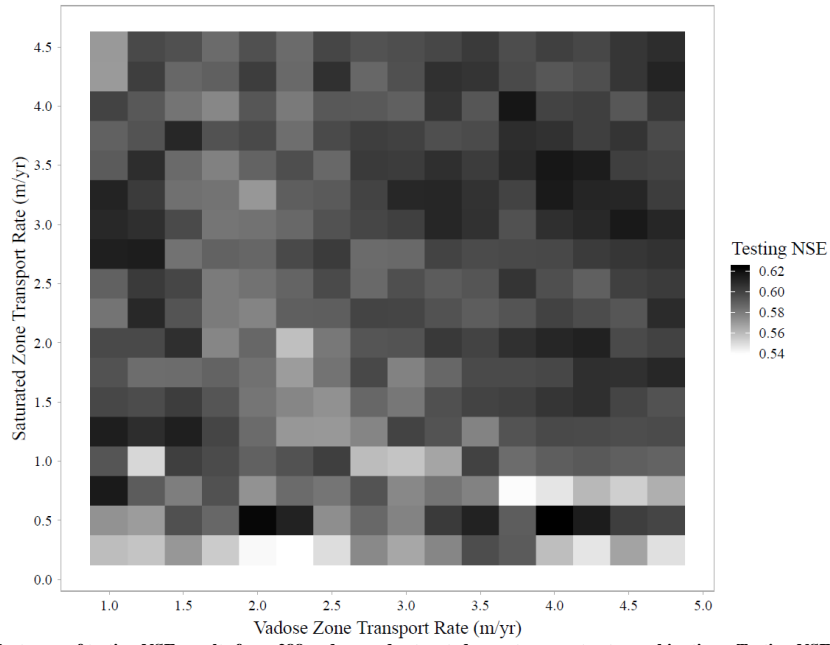


819  
 820 **Figure 2: Cross-section along representative well transect (see Fig. 1) within the Dutch Flats area. Surface elevation data**  
 821 **were derived from a 30-meter Digital Elevation Model (USGS, 1997). Water surface and base of aquifer elevations were**  
 822 **sourced from a 1998 Dutch Flats study (Böhlke et al., 2007, Verstraeten et al., 2001a, 2001b). Small black arrows beneath**  
 823 **the surface indicate general groundwater flow direction.**  
 824



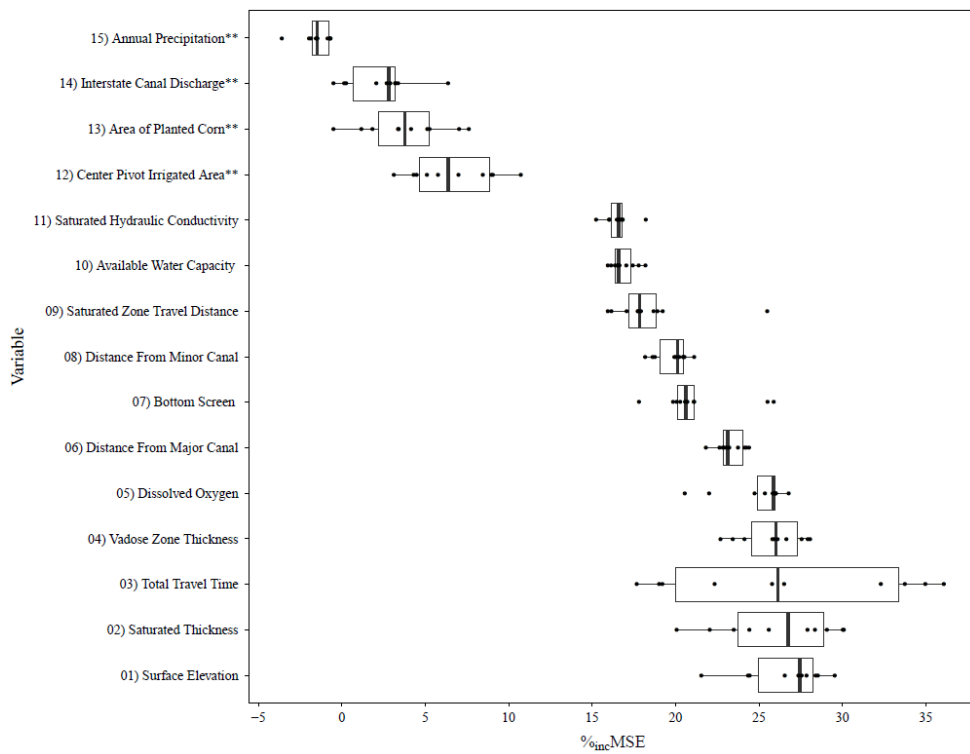
826  
827 **Figure 3: Time series plots of all four dynamic predictors. Figures represent (a) annual precipitation, (b) Interstate canal discharge, (c)**  
828 **center pivot irrigated area, and (d) area of planted corn from 1946 to 2013.**

830

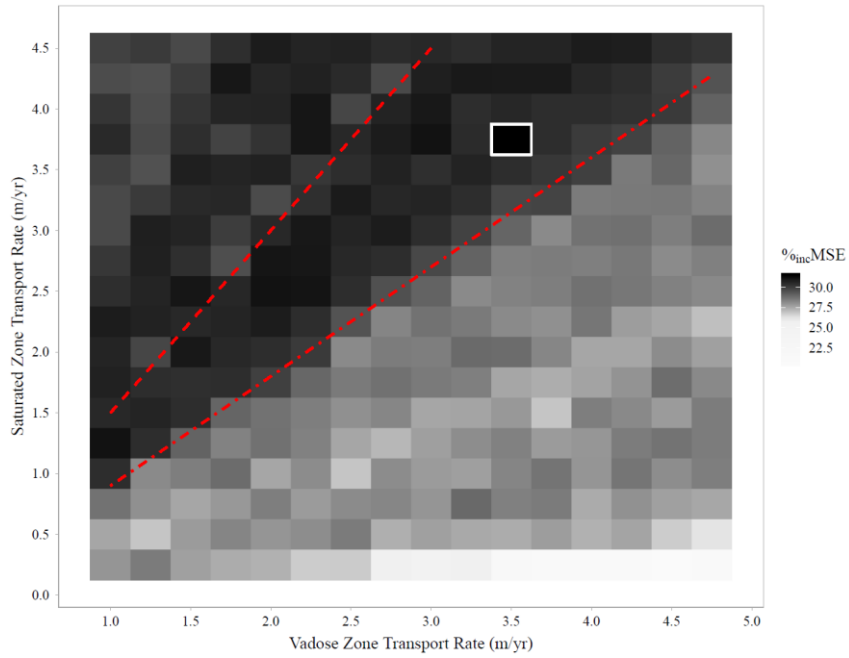


831  
832 **Figure 4: Heat map of testing NSE results from 288 vadose and saturated-zone transport rate combinations. Testing NSE in this figure**  
833 **is the median of all 25 model outputs from each of the 288 transport rate combinations. No clear pattern of optimal vadose and saturated-**  
834 **zone transport rate combinations was observed.**



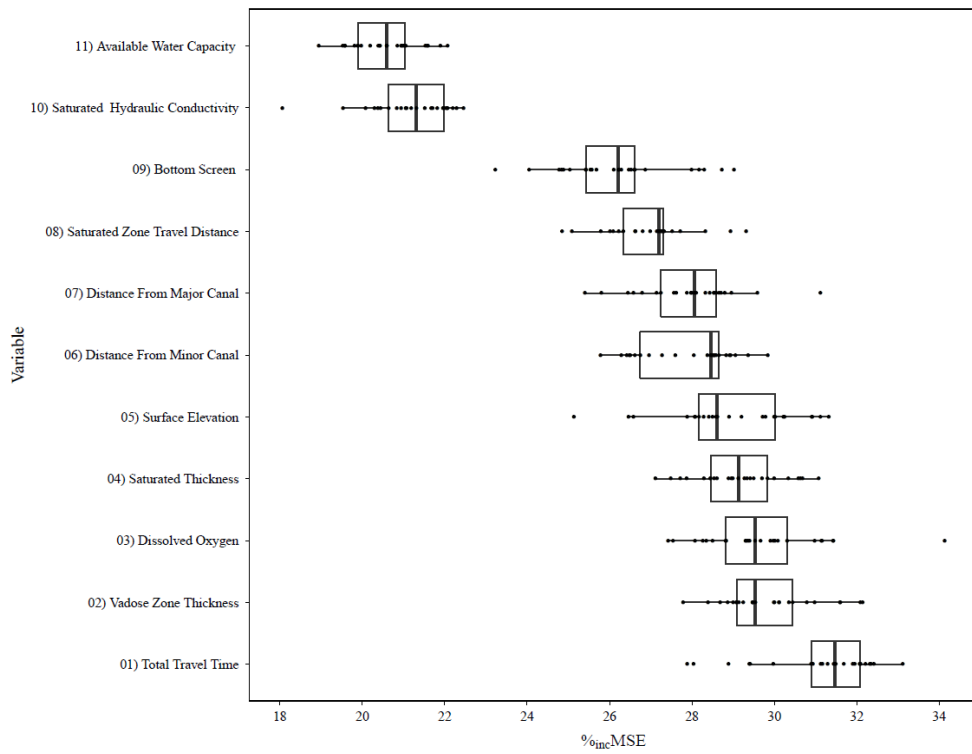


835  
 836 **Figure 5: Boxplot of the %incMSE from the ten transport rate combinations shown in Table 2. Each boxplot has ten points for each**  
 837 **transport rate combination, representing the median %incMSE from the 25 models (five-fold cross validation, repeated 5 times). A larger**  
 838 **%incMSE suggests the variable had a greater influence on a model's ability to predict [NO<sub>x</sub>]. \*\*Denotes dynamic predictors.**



839  
 840 **Figure 6: Heat map of %incMSE (median from 25 models) from variable importance of total travel time for each of the 288 transport**  
 841 **rate combinations evaluated. Red dashed lines indicate upper ( $V_w - Y_s / V_u = 1.5$ , long dashes) and lower (0.9, short dashes) bounds of the**  
 842 **band of transport rate combinations with consistently higher %incMSE. The white square highlights the single transport rate**  
 843 **combination with the highest %incMSE.**

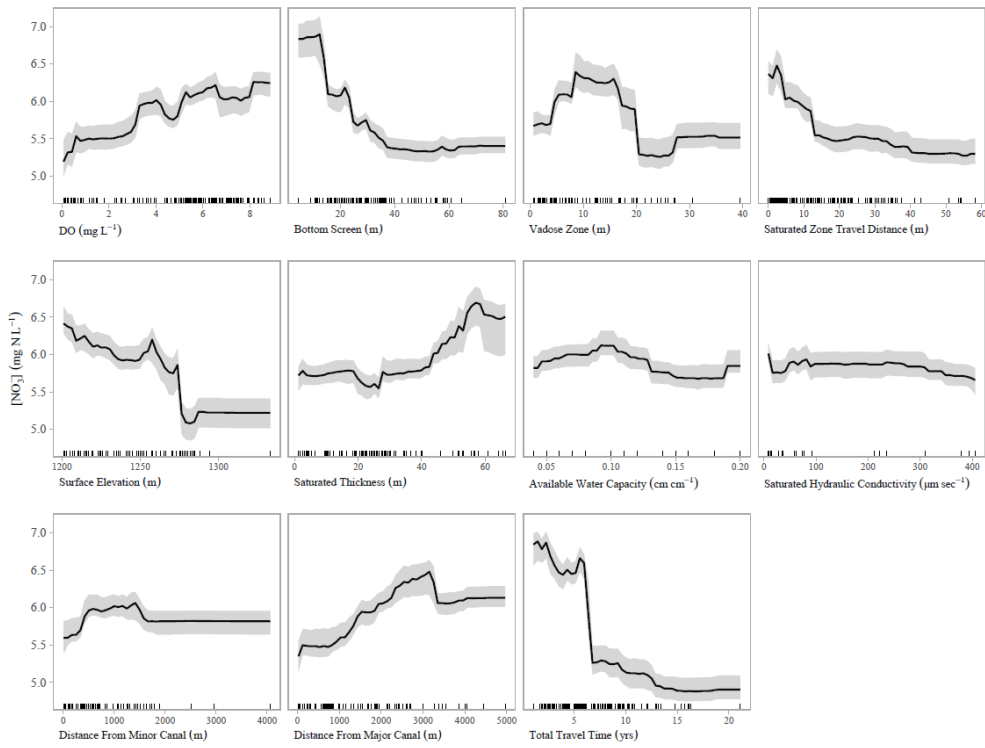
844



845  
 846 **Figure 7: Plot from secondary analysis exploring variable importance of the transport rate combination with the largest median**  
 847 **%incMSE in total travel time ( $V_u = 3.5$  m/yr;  $V_s = 3.75$  m/yr). Each point is from one of 25 Random Forest models run for this evaluation.**  
 848 **A larger %incMSE suggests the variable had a greater influence on a model's ability to predict  $[NO_3^-]$ .**

849

850



851 **Figure 8: Partial dependence plot for model evaluating transport rate combination of  $V_u = 3.5$  m/yr and  $V_s = 3.75$  m/yr. Tick marks on**  
 852 **each plot represent predictor observations used to train models.**  
 853

854

855

856

857

858

859

860

861

862

863

864 **Table 1. List of the 15 predictors used for Random Forest evaluation. Average (avg.) and median (med.) values are shown.**

Predictor	Units	Predictor Type	Source
Center Pivot Irrigated Area (avg. = 2618; med. = 1037) <sup>a</sup>	hectare	Dynamic	NAIP; NAPP; Landsat-1, 5, 7, 8 <sup>b</sup>
Interstate Canal Discharge (avg. = 0.53; med. = 0.55) <sup>a</sup>	km <sup>3</sup> yr <sup>-1</sup>	Dynamic	USBR (2018)
Area of Planted Corn (avg. = 8065; med. = 7869) <sup>a</sup>	hectare	Dynamic	NASS (2018)
Precipitation (avg. = 384; med. = 377) <sup>a</sup>	mm yr <sup>-1</sup>	Dynamic	NOAA (2017)
Available Water Capacity (avg. = 0.1; med. = 0.1)	cm cm <sup>-1</sup>	Static	NRCS (2018)
Dissolved Oxygen (avg. = 4.6; med. = 5.4)	mg L <sup>-1</sup>	Static	C. Hudson, Personal Communication (2018)
Distance from a Major Canal (avg. = 1462.2; med. = 1161.4)	m	Static	USGS (2012) <sup>b</sup>
Distance from a Minor Canal (avg. = 633.2; med. = 397.6)	m	Static	USGS (2012) <sup>b</sup>
Bottom Screen (avg. = 26.9; med. = 24.4)	m	Static	UNL (2016) <sup>b</sup>
Saturated Hydraulic Conductivity (avg. = 68; med. = 28)	μm sec <sup>-1</sup>	Static	NRCS (2018)
Saturated Thickness (avg. = 30.2; med. = 27.6)	m	Static	T. Preston, Personal Communication (2017) <sup>b</sup>
Saturated-Zone Travel Distance (avg. = 13.3; med. = 7)	m	Static	UNL (2016) <sup>b</sup>
Surface Elevation (DEM) (avg. = 1244; med. = 1248)	m	Static	USGS (1997)
Total Travel Time (avg. = 6.4; med. = 5.7) <sup>c</sup>	years	Static	UNL (2016) <sup>b</sup>
Vadose-Zone Thickness (avg. = 9.9; med. = 7.3)	m	Static	T. Preston, Personal Communication (2017); A. Young, Personal Communication (2016)

<sup>a</sup> Average and median span from 1946 to 2013

<sup>b</sup> Data required further analysis to yield calculated values; data sources are USDA (2017) and USGS (2017)

<sup>c</sup> Average and Median reflects transport rates of  $V_a = 3.5$  m/yr and  $V_u = 3.75$  m/yr

865

866 **Table 2. Summary of ten vadose and saturated-zone transport rate combinations selected from 288 unique potential combinations from**  
 867 **the analysis including dynamic variables.**

	Vadose-zone Transport Rate (m/yr)	Sat. Zone Transport Rate (m/yr)	Test NSE	[NO <sub>3</sub> ] <sup>-</sup> Observations <sup>a</sup>	Total Travel Time (yrs)	
					Mean ( $\pm 1\sigma$ )	Median
Five Top-Performing Transport Rates	4.00	0.50	0.623	878	19.9 ( $\pm 15.8$ )	11.3
	2.00	0.50	0.622	861	21.6 ( $\pm 15.0$ )	16.5
	3.75	4.00	0.617	1049	6 ( $\pm 3.7$ )	5.4
	4.00	3.50	0.617	1049	6.3 ( $\pm 4.1$ )	5.7
	4.50	3.00	0.616	1049	6.7 ( $\pm 4.7$ )	5.7
Extreme and Midrange Transport Combinations	4.75	4.50	0.608	1049	5.1 ( $\pm 3.2$ )	4.6
	2.75	2.25	0.599	1049	9.6 ( $\pm 6.3$ )	8.5
	1.00	4.50	0.570	1049	12.6 ( $\pm 7.7$ )	10.8
	1.00	0.25	0.559	607	26.7 ( $\pm 13.3$ )	20.6
	4.75	0.25	0.548	664	21.3 ( $\pm 15.0$ )	14.9

868 <sup>a</sup>In cases with slow transport rates, lag times were relatively long and not all [NO<sub>3</sub>]<sup>-</sup> data could be used in the model. For example, a slow transport rate combination  
 869 resulting in a lag time with the infiltration year prior to 1946 could not be included. Thus, some models were ultimately based on <1,049 observations.